Accepted Manuscript

Cationic biaryl 1,2,3-triazolyl peptidomimetic amphiphiles: Synthesis, antibacterial evaluation and preliminary mechanism of action studies

Andrew J. Tague, Papanin Putsathit, Katherine A. Hammer, Steven M. Wales, Daniel R. Knight, Thomas V. Riley, Paul A. Keller, Stephen G. Pyne

PII: S0223-5234(19)30123-0

DOI: https://doi.org/10.1016/j.ejmech.2019.02.013

Reference: EJMECH 11105

To appear in: *European Journal of Medicinal Chemistry*

Received Date: 28 November 2018

Revised Date: 18 January 2019

Accepted Date: 4 February 2019

Please cite this article as: A.J. Tague, P. Putsathit, K.A. Hammer, S.M. Wales, D.R. Knight, T.V. Riley, P.A. Keller, S.G. Pyne, Cationic biaryl 1,2,3-triazolyl peptidomimetic amphiphiles: Synthesis, antibacterial evaluation and preliminary mechanism of action studies, *European Journal of Medicinal Chemistry* (2019), doi: https://doi.org/10.1016/j.ejmech.2019.02.013.

Graphical Abstract – EurJMedChem

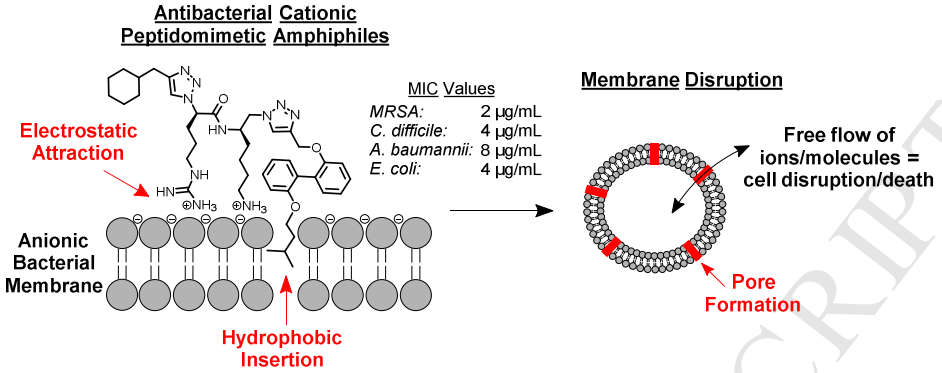

Cationic biaryl 1,2,3-triazolyl peptidomimetic amphiphiles: synthesis, antibacterial evaluation and preliminary mechanism of action studies

Andrew J. Tague[a†], Papanin Putsathit[b], Katherine A. Hammer[c], Steven M. Wales[a], Daniel R. Knight[d], Thomas V. Riley[b,c,d,e], Paul A. Keller[a†] and Stephen G. Pyne[a†]

[a]*School of Chemistry, University of Wollongong, Wollongong, NSW 2522, Australia*
[b]*School of Medical and Health Sciences, Edith Cowan University, Western Australia 6027, Australia*
[c]*School of Biomedical Sciences, The University of Western Australia, Western Australia 6009, Australia*
[d]*School of Veterinary and Life Sciences, Murdoch University, Western Australia 6150, Australia*
[e]*PathWest Laboratory Medicine, Queen Elizabeth II Medical Centre, Western Australia 6009, Australia*

[†] Corresponding authors: atague@uow.edu.au (A. Tague)
keller@uow.edu.au (P. Keller)
spyne@uow.edu.au (S. Pyne)

Abstract

Synthetic small molecular antimicrobial peptidomimetics represent a promising new class of potential antibiotics due to their membrane-disrupting ability and their decreased propensity for bacterial resistance. A library of 43 mono- and di-cationic biaryl 1,2,3-triazolyl peptidomimetics was designed and synthesized based upon previously established lead biarylpeptidomimetics and a known pharmacophore. A reliable, facile and modular synthetic pathway allowed for the efficient synthesis of multiple unique scaffolds which were subjected to divergent derivatization to furnish the amphiphilic compounds. *In vitro* testing revealed enhanced antibacterial efficacy against a range of pathogenic bacteria, including bacterial isolates with methicillin, vancomycin, daptomycin, or multi-drug resistance. Preliminary time-kill kinetics and membrane-disruption assays revealed a likely membrane-active mechanism for the tested peptidomimetics. An optimal balance between hydrophobicity and cationic charge was found to be essential for reduced cytotoxicity/haemolysis (i.e. membrane selectivity) and enhanced Gram-negative activity. The cationic biaryl amphiphile **81** was identified as a potent, broad-spectrum peptidomimetic with activity against Gram-positive (methicillin-resistant *Staphylococcus aureus* - MIC = 2 µg/mL) and Gram-negative (*Escherichia coli* - MIC = 4 µg/mL) pathogenic bacteria.

Keywords:
Antibacterial
Peptidomimetic
Biaryl cationic amphiphiles
Membrane depolarization
Amphipathic

1. Introduction

The emergence and increasing prevalence of bacterial resistance to modern anthropogenic antibiotics has been identified as a global healthcare crisis and drug resistant bacterial infections have been categorized as an "emergent global disease" by the World Health Organization (WHO) and the US Centers for Disease Control and Prevention (CDC) [1-4]. Infectious disease is the second leading killer globally (17 million deaths annually) and the CDC estimates that antibacterial resistance is responsible for two million infections and 23,000 deaths in the USA per annum [2, 5]. Multi-drug resistant (MDR) organisms are particularly concerning and the **ESKAPE** pathogens (i.e. ***E****nterococcus faecium*, ***S****taphylococcus aureus*, ***K****lebsiella pneumoniae*, ***A****cinetobacter baumannii*, ***P****seudomonas aeruginosa* and ***E****nterobacter* spp.) are six antibiotic resistant bacteria that have been identified by multiple agencies, including the Infectious Diseases Society of America (IDSA), as key pathogens behind the majority of nosocomial infections [6]. These bacteria have been identified due to their virulence, tenacity, propensity for resistance and pathogenicity [6]. There currently exists an urgent unmet need for novel antibiotic chemotherapeutics to combat MDR bacterial infections and the IDSA has instituted the "10 by '20" Initiative, which aims to facilitate the discovery and development of 10 novel antibiotics drugs by the year 2020 [3, 5, 7].

Antimicrobial peptides (AMPs) are found in a wide array of organisms where they provide a natural defence against invading microbial pathogens [8]. These peptides are typically cationic and amphiphilic in nature because they contain basic amino acids (cationic at physiological pH) and a high percentage (>50%) of hydrophobic side chain residues [9-10]. The cationic residues allow for electrostatic attraction to the anionic bacterial membrane while the hydrophobic residues insert into the lipophilic interior of the lipid bilayer membrane; this ultimately results in disruption of the membrane integrity and can lead to cell death [8-10]. AMPs are generally thought to exhibit a reduced propensity for bacterial resistance due to their unique mode of action (i.e. cellular membrane disruption) [9]; despite this, acquired resistance to AMPs and small molecular peptidomimetics has been documented [10-11]. Unfortunately, most naturally occurring AMPs have limited applicability due to their *in vivo* toxicity (i.e. lack of membrane selectivity), high manufacturing costs and their susceptibility to protease metabolism [9, 12-13]. Recent developments in small molecular AMP mimics aim to eliminate these limitations [12-21]. One successful example is LTX-109, a three-residue AMP mimic by Lytix Biopharma that has completed Phase 2 clinical trials as a topical agent for nasal decolonization of MRSA [22-23].

Most AMP mimics are non-selective towards cellular membranes and thus exhibit haemolytic and cytotoxic activity against mammalian cells. Small molecular AMP mimics often display a positive correlation between antibacterial activity and cytotoxicity due to their non-selective membrane disrupting ability, which precludes these molecules from becoming effective systemic antimicrobial drugs [24]. Fine-tuning the membrane selectivity to target bacterial membranes over eukaryotic membranes will be essential for the development of an effective membrane-disrupting, systemically administered antibiotic. Liu and co-workers [16] have successfully explored the hydrophobic/cationic balance in xanthone derivatives, developing compounds that exhibit virtually no haemolysis while maintaining potent antibacterial activity against Gram-positive bacteria. Antibacterial efficacy against Gram-negative bacteria is ultimately needed, as many of the resistant pathogenic bacteria, such as the **ESKAPE** pathogens, are Gram-negative (e.g. *K. pneumoniae*, *A. baumannii* and *P. aeruginosa*) [6, 25].

Previous work in our laboratory has produced a promising class of biaryl cationic peptidomimetics that exhibit antimicrobial activity against a broad range of Gram-positive and Gram-negative pathogenic bacteria, including the problematic *Clostridium difficile* and bacterial strains that are resistant to methicillin, vancomycin and linezolid [14-15, 26-29]. The systemic and topical antibacterial efficacy of these compounds has been demonstrated *in vivo* with methicillin-resistant *S. aureus* (MRSA) infection models in mice [26]. Recent studies have led to the development of peptidomimetic compound **1**, which incorporates a 1,2,3-triazole moiety as a protease-resistant peptide bioisostere; this derivative was also shown to exhibit potent minimum inhibitory concentration (MIC) values against Gram-positive and Gram-negative bacteria (Fig. 1) [14]. The biaryl cationic peptidomimetics conform to a simple, preliminary pharmacophore model [14] that comprises a biaryl aromatic core with attached cationic residues and hydrophobic residues; this confers an amphiphilic structure to the compounds which is essential for antibacterial efficacy. This pharmacophore is analogous to other AMP mimic models, such as those proposed by Haldar *et al.* [12] and Kumar *et al.* [13]; further elucidation of the essential components for broad-spectrum antibacterial efficacy and membrane selectivity will allow for the rational design of potent and selective AMP mimics for potential use as chemotherapeutic agents.

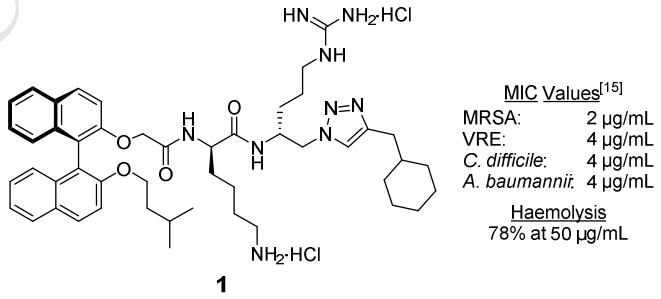

1

Fig. 1. Lead peptidomimetic compound **1**.

In this current study, lead compound **1** was structurally modified to obtain novel AMP mimics with increased solubility and antibacterial efficacy against Gram-negative bacteria. Modification strategies included further

incorporation of peptidomimetic 1,2,3-triazole moieties for enhanced metabolic stability, replacement of the binaphthalene aromatic core with the more soluble biphenyl moiety and manipulation of the cationic/hydrophobic residue arrangements. These modifications allowed for the synthesis of 43 novel biaryl cationic peptidomimetics with significant antibacterial activity against various pathogenic Gram-positive and Gram-negative bacteria. Additionally, selected derivatives were subjected to time-kill kinetics and membrane disruption assays to investigate the antibacterial mode of action. Haemolysis and *in vitro* cytotoxicity assays were utilized to identify any eukaryotic cytotoxicity.

2. Results and Discussion

2.1. Design, synthesis and characterization of cationic biaryl peptidomimetic amphiphiles

Three distinct classes of cationic biaryl 1,2,3-triazolyl amphiphiles were designed and synthesized for antibacterial evaluation: monocationic terminal amide analogues (**A**), dicationic terminal amide analogues (**B**) and dicationic bis-triazole derivatives (**C**) (Fig. 2).

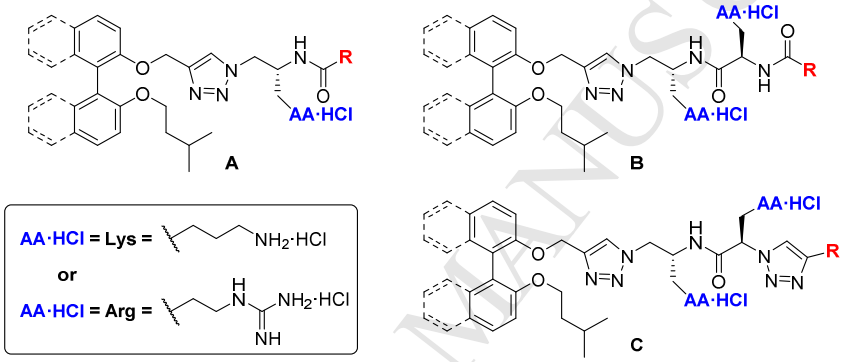

Fig. 2. General structures of the cationic biaryl 1,2,3-triazolyl peptidomimetic amphiphiles (Series **A**, **B** and **C**) synthesized in this study.

Previous investigations established the efficacy of 1,2,3-triazole moieties as bioisosteric amide bond replacements in the biaryl cationic amphiphiles (e.g. lead compound **1**) [14]. Therefore, the biaryl amide linker in lead compound **1** was targeted for bioisosteric triazole substitution; subsequent variation of the biaryl core (i.e. (*S*)-binaphthyl or biphenyl), cationic amino acid residues (i.e. Lys and/or Arg) and the hydrophobic termini linker (i.e. amide or 1,2,3-triazole) led to the development of Series **A**, **B** and **C** peptidomimetics. The unnatural *D*-configured amino acids were utilized as they have been shown to confer increased metabolic stability to AMPs [30].

A modular synthetic approach was employed for the construction of multiple unique peptidomimetic scaffolds from key azide, alkyne, acid and amine building blocks. Cu-catalysed azide-alkyne cycloaddition (CuAAC) and peptide coupling reactions were exploited to assemble the various scaffolds, as exemplified in Scheme 1. The terminal amine or azide scaffolds (e.g. compound **7** or **10**) served as divergence points from which multiple antimicrobial derivatives were realized. The hydrophobic termini were installed *via* peptide coupling or CuAAC reaction; subsequent acidolytic deprotection of the cationic side-chains furnished the final compounds as mono- or di-hydrochloride salts (e.g. compounds **A** and **C**).

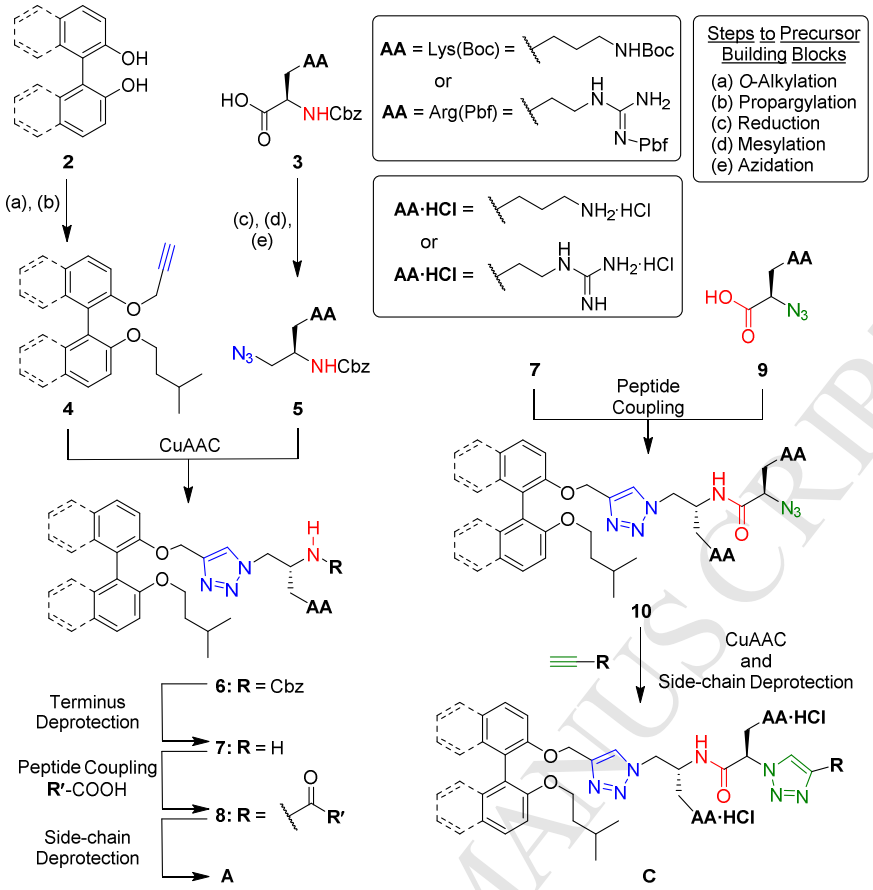

Scheme 1. Modular synthetic strategy utilized to achieve Series **A** and Series **C** derivatives.

The biphenyl (**15**) and (*S*)-binaphthyl (**16**) alkyne building blocks were obtained in excellent yield *via* sequential *O*-alkylation [27-28, 31] and *O*-propargylation reactions of the commercially available 2,2′-biphenol (**11**) or 2,2′-binaphthol (**12**) starting materials (Scheme 2).

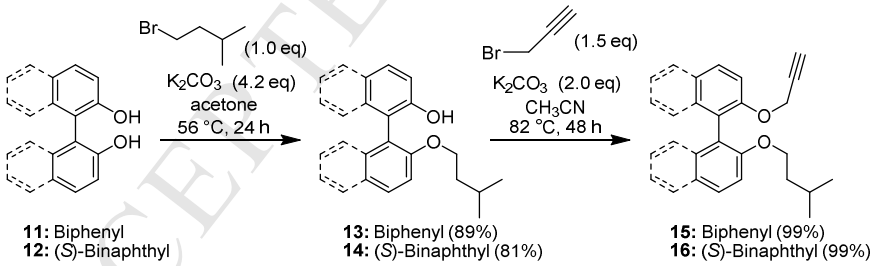

Scheme 2. Synthesis of precursor alkynes **15** and **16**.

The required azido amine precursors were constructed from commercially available D-amino acids. Mixed anhydride reduction of the *N*-Cbz amino acids (**17** and **18**) furnished the corresponding alcohols (**19** and **20**) which were then subjected to a two-step, one-pot mesylation/azidation reaction sequence to yield the *N*-Cbz azido amine building blocks **21** and **22** (Scheme 3). Azido acids **25** and **26** were synthesized *via* diazotransfer reaction of the corresponding D-amino acids (Scheme 4a) and the *N*-Boc azido amine **28** was realized by reaction of the known β-azido-amine **27** [14] with Boc_2O (Scheme 4b).

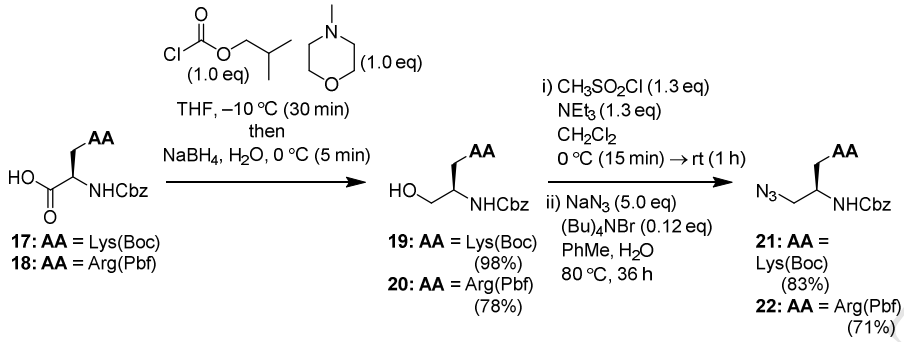

Scheme 3. Synthesis of *N*-Cbz azido amines **21** and **22**.

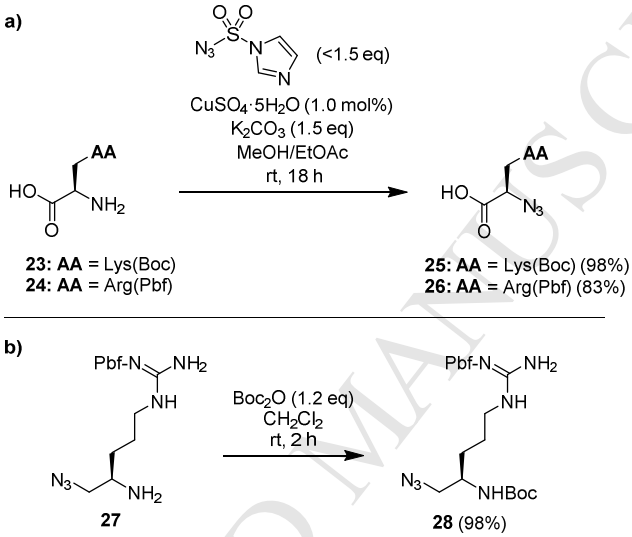

Scheme 4. Azide precursors: **a)** Synthesis of azido acids **25** and **26**. **b)** Synthesis of *N*-Boc-*β*-azido-amine **28**.

The *N*-protected Series **A** scaffold intermediates (**29–33**) were constructed by CuAAC reactions between the corresponding aromatic alkyne (**15** or **16**) and azide (**21**, **22** or **28**) precursor building blocks (Scheme 5). The sterically hindered (*S*)-binaphthyl analogues **31–33** required an increased reaction temperature (45 °C) to furnish the desired 1,2,3-triazole products. The 1,4-regioselectivity of the CuAAC reaction [32-34] was elucidated by analysis of the gHMBC NMR spectrum of the resultant *N*-deprotected scaffold amine **34** (Fig. S23).

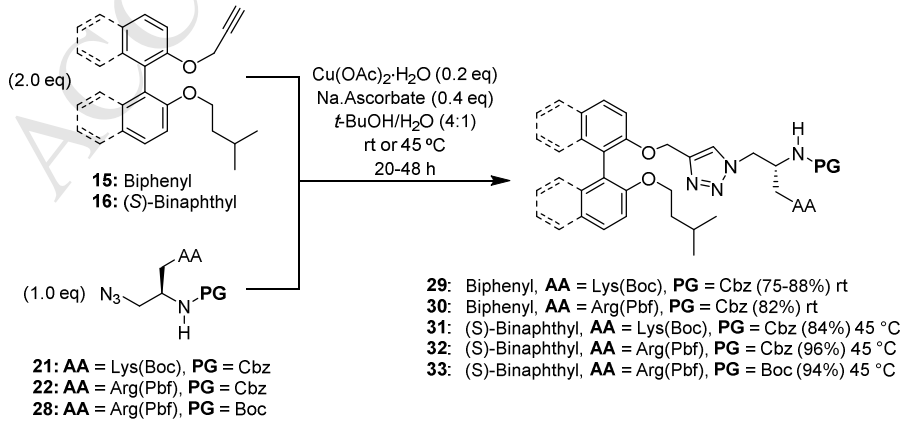

Scheme 5. Synthesis of the Series **A** scaffold intermediates.

Terminal group deprotection of the *N*-Cbz intermediates **29–31** by catalytic hydrogenolysis over Pd/C and H_2 gas gave access to scaffold amines **34–36**, while the *N*-Boc scaffold **33** was subjected to mild acidolytic conditions *via* anhydrous HCl in MeOH/Et_2O to achieve scaffold amine **37** without removal of the more robust *N*-Pbf moiety (Scheme 6).

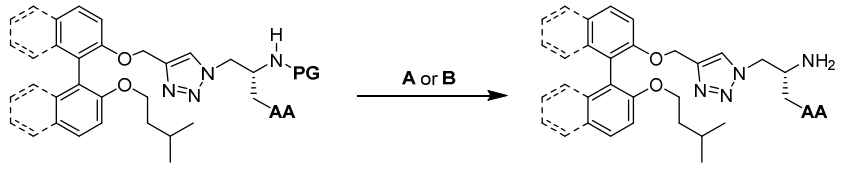

29: Biphenyl, **AA** = Lys(Boc), **PG** = Cbz
30: Biphenyl, **AA** = Arg(Pbf), **PG** = Cbz
31: (*S*)-Binaphthyl, **AA** = Lys(Boc), **PG** = Cbz
33: (*S*)-Binaphthyl, **AA** = Arg(Pbf), **PG** = Boc

34: Biphenyl, **AA** = Lys(Boc), Rxn **A** (99%)
35: Biphenyl, **AA** = Arg(Pbf), Rxn **A** (92%)
36: (*S*)-Binaphthyl, **AA** = Lys(Boc), Rxn **A** (98%)
37: (*S*)-Binaphthyl, **AA** = Arg(Pbf), Rxn **B** (95%)

Scheme 6. Synthesis of Series **A** amine scaffolds *via* terminal *N*-deprotection. **Reagents and conditions: A**) 10% Pd-C (0.15 eq), H_2 (1 atm), AcOH (20.0 eq), MeOH, rt, 24 h; **B**) HCl (20.0 eq), MeOH, rt, 18 h.

Derivatization of the Series **A** scaffold amines (**34–37**) was accomplished by EDCI/HOBt promoted amide bond formation with various hydrophobic carboxylic acids (**R**-COOH) in CH_3CN; acidolytic *N*-deprotection of the cationic side-chains with TFA/CH_2Cl_2/H_2O followed by treatment with HCl/Et_2O yielded the Series **A** monocationic amphiphiles **38–63** (Table 1) as their hydrochloride salts.

Table 1. Synthesis of the Series **A** monocationic amphiphiles.

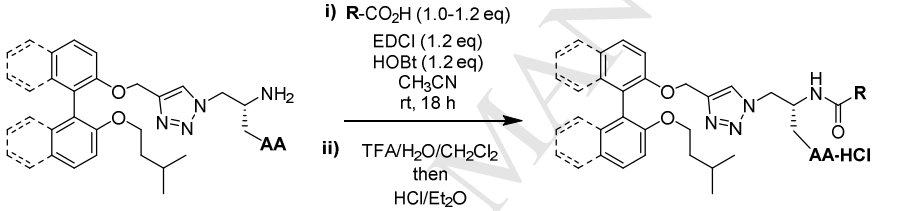

34: Biphenyl, **AA** = Lys(Boc)
35: Biphenyl, **AA** = Arg(Pbf)
36: (*S*)-Binaphthyl, **AA** = Lys(Boc)
37: (*S*)-Binaphthyl, **AA** = Arg(Pbf)

38–40: Biphenyl, **AA·HCl** = Lys
41–43: Biphenyl, **AA·HCl** = Arg
44–60: (*S*)-Binaphthyl, **AA·HCl** = Lys
61–63: (*S*)-Binaphthyl, **AA·HCl** = Arg

Entry	Compound	**Aromatic Core**	**AA·HCl**	**R**	Yield(%)[a]
1	**38**	Biphenyl	Lys	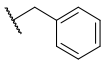	96
2	**39**	Biphenyl	Lys	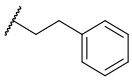	93
3	**40**	Biphenyl	Lys	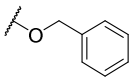	93[b]
4	**41**	Biphenyl	Arg	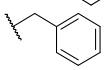	84
5	**42**	Biphenyl	Arg	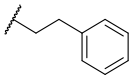	95
6	**43**	Biphenyl	Arg	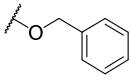	87[b]
7	**44**	(*S*)-Binaphthyl	Lys	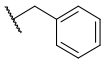	95
8	**45**	(*S*)-Binaphthyl	Lys	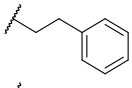	82
9	**46**	(*S*)-Binaphthyl	Lys	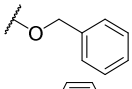	99[b]
10	**47**	(*S*)-Binaphthyl	Lys		85

11	**48**	(*S*)-Binaphthyl	Lys	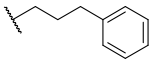	82
12	**49**	(*S*)-Binaphthyl	Lys	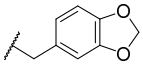	85
13	**50**	(*S*)-Binaphthyl	Lys	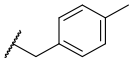	67
14	**51**	(*S*)-Binaphthyl	Lys	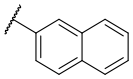	90
15	**52**	(*S*)-Binaphthyl	Lys	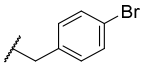	77
16	**53**	(*S*)-Binaphthyl	Lys		67
17	**54**	(*S*)-Binaphthyl	Lys		73
18	**55**	(*S*)-Binaphthyl	Lys		88
19	**56**	(*S*)-Binaphthyl	Lys		86
20	**57**	(*S*)-Binaphthyl	Lys		74
21	**58**	(*S*)-Binaphthyl	Lys		86
22	**59**	(*S*)-Binaphthyl	Lys	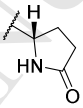	85
23	**60**	(*S*)-Binaphthyl	Lys	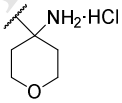	88
24	**61**	(*S*)-Binaphthyl	Arg	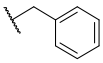	86
25	**62**	(*S*)-Binaphthyl	Arg	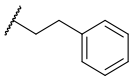	89
26	**63**	(*S*)-Binaphthyl	Arg	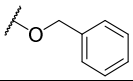	96[b]

[a] Yields are reported over two steps.
[b] Synthesised in one step from the corresponding *N*-Cbz protected scaffold intermediate.

Series **B** scaffold amines **64** and **65** were synthesized from scaffold amine **34** or **36** by EDCI/HOBt peptide coupling with Fmoc-(*D*)-Arg(Pbf)-OH followed by base-promoted *N*-Fmoc deprotection (Scheme 7). Derivatization of the Series **B** scaffold amines was accomplished by the general peptide coupling/side-chain deprotection sequence, thus furnishing the Series **B** dicationic amphiphiles **68–74** (Table 2) as their di-hydrochloride salts.

The Series **C** scaffold azides **75–77** were assembled from scaffold amines **34–36** by EDCI/HOBt peptide coupling with the corresponding azido acid precursor (**25** or **26**) (Scheme 8). The resultant azides were then subjected to derivatization *via* sequential CuAAC reaction and acidolytic side-chain deprotection to achieve the Series **C** dicationic amphiphiles **78–87** (Table 3) as their di-hydrochloride salts.

The employed synthetic methodology was amenable to scale-up; compounds **80** and **81** were prepared in >1 gram quantities (for *in vivo* assays) and their purity was confirmed (>97%) by reverse-phase analytical HPLC (Fig. S28 and S29).

Notably, some of the synthesized amphiphilic peptidomimetics (e.g. compounds **40** and **81**) failed to display ^{13}C NMR resonances that could be assigned to the quaternary triazole carbons when the spectra were acquired in $CDCl_3$ or CD_3OD; for instance, compound **81** required gHMBC correlations with the adjacent triazole methine protons to allow for assignment of both quaternary triazole carbons (Fig. S24). gHMBC analysis did not show

the relevant correlations for compound **40** when the spectrum was acquired in CD_3OD; the ^{13}C DEPT Q NMR spectrum had to be acquired in DMSO-d_6 for the requisite carbon resonance to be clearly visible.

The presence of carbamate and amide rotamers was observed in the ^{1}H and ^{13}C NMR spectra of particular derivatives. Compound **40** was found to exhibit rotameric shouldering in the ^{1}H NMR spectrum (Fig. S25) and similar rotameric "shoulder" resonances in the ^{13}C NMR spectrum (Fig. S26). The presence of *syn*- and *anti*-rotamers was confirmed by variable temperature NMR experiments; the observed resonance splitting in the ^{13}C NMR spectrum of compound **40** was reduced when the spectrum was acquired in DMSO-d_6 and the splitting was completely eliminated when the ^{13}C NMR spectrum was acquired in DMSO-d_6 at 90 °C (Fig. S27).

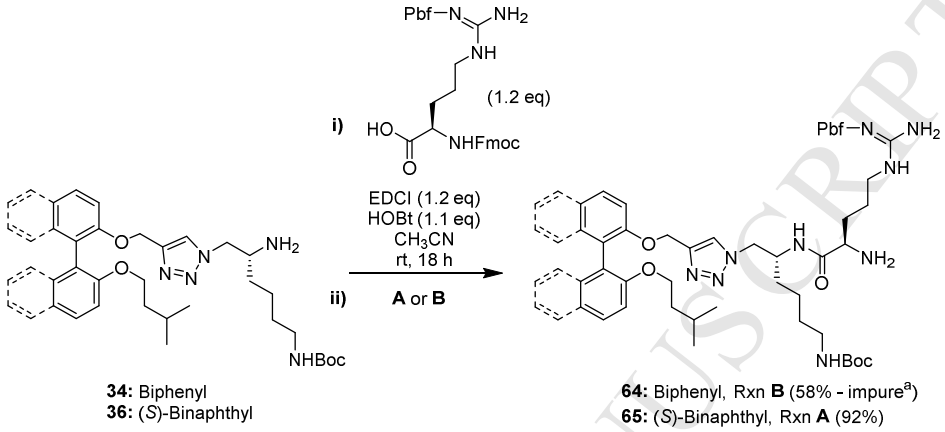

Scheme 7. Synthesis of the Series **B** amine scaffolds **64** and **65**. **Reagents and conditions: A**) Piperidine (5.0 eq), CH_3CN, rt, 18 h; **B**) tris-(2-aminoethyl)amine (5.0 eq), CH_3CN, rt, 18 h. [a] By-products from *N*-Fmoc deprotection reaction.

Table 2. Synthesis of the Series **B** dicationic amphiphiles.

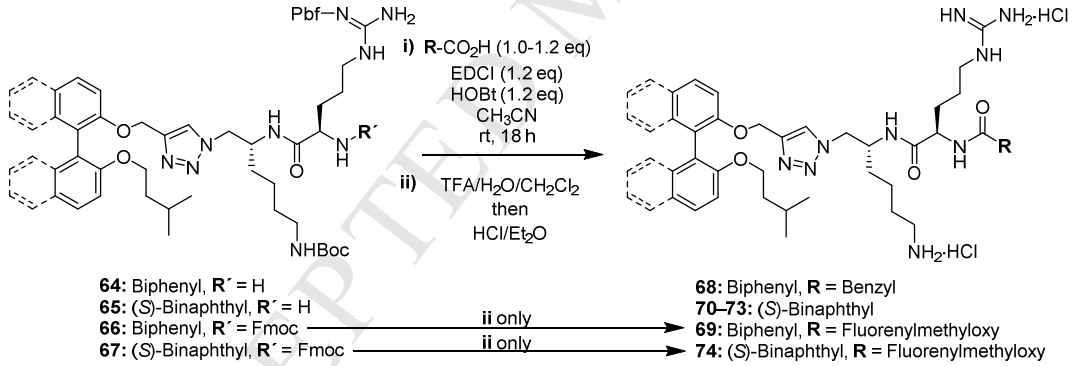

Entry	Compound	**Aromatic Core**	**R**	Yield(%)[a]
1	**68**	Biphenyl	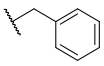	61%[b]
2	**69**	Biphenyl	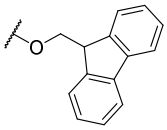	95%[c]
3	**70**	(*S*)-Binaphthyl	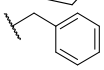	73%
4	**71**	(*S*)-Binaphthyl	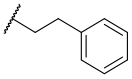	77%
5	**72**	(*S*)-Binaphthyl	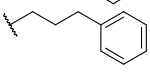	79%
6	**73**	(*S*)-Binaphthyl	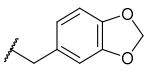	86%

7	**74**	(*S*)-Binaphthyl	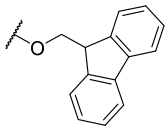	85%[c]

[a] Yields are reported over two steps.
[b] Yield is reported over four steps from scaffold amine **34**.
[c] Synthesised in one step from the corresponding *N*-Fmoc protected scaffold intermediate.

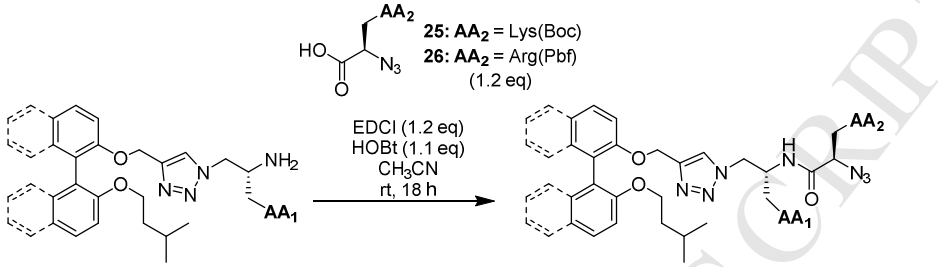

Scheme 8. Synthesis of the Series **C** azide scaffolds **75**–**77**.

Table 3. Synthesis of the Series **C** dicationic amphiphiles.

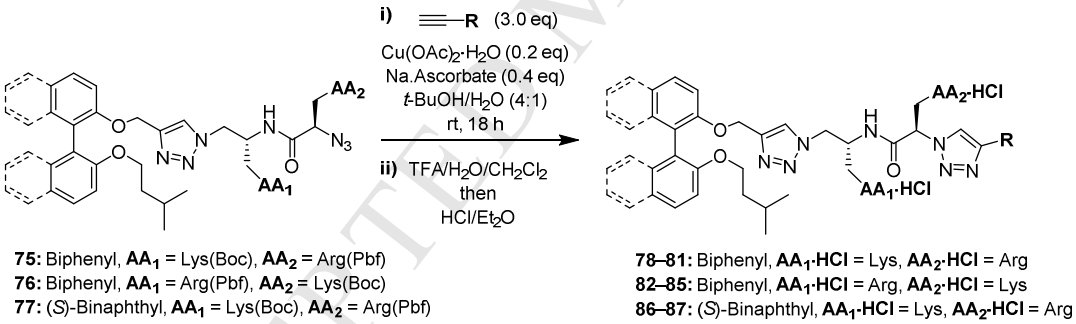

Entry	Compound	**Aromatic Core**	**AA_1·HCl**	**AA_2·HCl**	**R**	Yield(%)[a]
1	**78**	Biphenyl	Lys	Arg	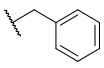	86
2	**79**	Biphenyl	Lys	Arg	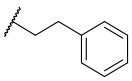	94
3	**80**	Biphenyl	Lys	Arg		92
4	**81**	Biphenyl	Lys	Arg	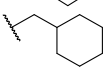	79
5	**82**	Biphenyl	Arg	Lys	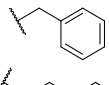	97
6	**83**	Biphenyl	Arg	Lys	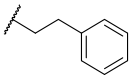	95
7	**84**	Biphenyl	Arg	Lys		84

8	**85**	Biphenyl	Arg	Lys	N/A[b]	97
9	**86**	(*S*)-Binaphthyl	Lys	Arg	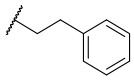	58
10	**87**	(*S*)-Binaphthyl	Lys	Arg	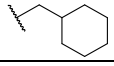	74

[a] Yields are reported over two steps.
[b] No terminal triazole moiety; synthesised by *N*-deprotection of the corresponding azide scaffold.

2.2. Antibacterial activity evaluation

The Series **A**, **B** and **C** peptidomimetic amphiphiles were screened in an *in vitro* MIC assay against a primary panel of Gram-positive pathogenic bacteria; vancomycin was used a positive control and the results are displayed in Tables 4, 5 and 6. Selected compounds were then tested against a secondary panel of pathogenic Gram-negative bacteria and MRSA at the Community for Open Antimicrobial Drug Discovery (CO-ADD) [35]. CO-ADD also performed a cytotoxicity concentration (CC_{50}) assay against the selected compounds at concentrations ≤32 µg/mL. Vancomycin, colistin and tamoxifen were used as positive controls in the Gram-positive, Gram-negative and cytotoxicity assays, respectively. The resultant CO-ADD antibacterial activities and CC_{50} values from Series **A**, **B** and **C** are displayed in Tables 7, 8 and 9, respectively. Additionally, four compounds (**41, 45, 71** and **73**) were tested against an extended panel of drug-resistant Gram-positive pathogens at CO-ADD with vancomycin and daptomycin as positive controls; the results are displayed in Table 10.

2.2.1. Series A derivatives

Primary screening results for the monocationic Series **A** derivatives (Table 4) indicated successful bioisosteric substitution of the biaryl amide linker with the 1,4-disubstituted-1,2,3-triazole moiety; the synthesized (*S*)-binaphthyl monocationic derivatives (**44**–**63**) exhibited significant antibacterial efficacy and most compounds displayed MIC values ranging from 4–8 µg/mL against *S. aureus*. The incorporation of bulky (e.g. naphthyl, compound **51**) and hydrophilic (e.g. 4-amino-tetrahydropyran-4-yl, compound **60**) terminal substituents led to a decrease in antibacterial efficacy against Gram-positive bacteria; compounds **51** and **60** exhibited less potent MIC values of 16 µg/mL against *S. aureus* (Table 4). (*S*)-binaphthyl derivatives **44**–**63** also exhibited antibacterial activity against *E. faecalis* (MIC = 8–16 µg/mL) with reduced antibacterial efficacy against *Staphylococcus pneumoniae* (MIC = 8–32 µg/mL) and *C. difficile* (MIC = 16–64 µg/mL). The (*S*)-binaphthyl monocationic arginine analogues **61–63** were notably more potent than their lysine counterparts (**44–46**), as they were the only monocationic (*S*)-binaphthyl analogues to exhibit strong antibacterial efficacy against *S. pneumoniae* (MIC = 8 µg/mL).

Replacement of the (*S*)-binaphthyl aromatic core with a biphenyl core did not adversely affect the antimicrobial efficacy of the monocationic amphiphiles. While a slight reduction in potency was observed for some analogues and Gram-positive strains (e.g. biphenyl compound **41** exhibits MIC values against *S. aureus* that are 4× less potent than its (*S*)-binaphthyl analogue **61**), an increase in potency was noted for other strains (e.g. biphenyl compound **41** exhibits MIC values against *C. difficile* PCR ribotype (RT) 027 that are 4× more potent than its (*S*)-binaphthyl analogue **61**) – see Table 4. The overall effect of aromatic core replacement on the antibacterial efficacy of the cationic amphiphiles was highly species dependent. Most notably, the biphenyl compounds **39** and **40** exhibited increased potency against *C. difficile* (MIC = 8 µg/mL) relative to their (*S*)-binaphthyl analogues **45** and **46** (MIC = 32 µg/mL). Furthermore, biphenyl derivatives **38** and **39** exhibited a 2–4× fold increase in activity against *S. pneumoniae* when compared to their (*S*)-binaphthyl analogues **44** and **45**. Secondary screening of selected Series **A** monocationic derivatives against Gram-negative pathogens and MRSA at CO-ADD further confirmed that replacement of the (*S*)-binaphthyl core with a biphenyl aromatic core resulted in a reduction of antibacterial potency against MRSA (Table 7). The selected monocationic derivatives were generally not active at the concentrations tested or only mildly active (MIC = 32 µg/mL) against the pathogenic Gram-negative bacteria (Table 7). Ultimately, compounds **39** and **62** were identified as the most promising derivatives from Series **A**, with MIC values ranging from 4–16 µg/mL for all tested Gram-positive bacterial strains.

2.2.2. Series B derivatives

The addition of a second cationic residue to give Series **B** dicationic terminal amides (**68–74**) led to a general increase in antibacterial efficacy; e.g. (*S*)-binaphthyl dicationic compounds **70** and **71** exhibited MIC values of 2 µg/mL against MRSA (Table 8). Notably, the antibacterial activity against all Gram-positive bacteria was increased for the Series **B** dicationic amides relative the Series **A** monocationic derivatives; MIC values as low as 2 µg/mL against *E. faecalis*, 4 µg/mL against *S. pneumoniae* and 8 µg/mL against *C. difficile* (ATCC 70057) were observed (Table 5). The Series **B** dicationic biphenyl analogues (**68** and **69**) exhibited similar antibacterial activities relative to the (*S*)-binaphthyl analogues **70–74**; biphenyl compound **68** was found to be approximately 2× less potent than its (*S*)-binaphthyl analogue **70**, whereas biphenyl compound **69** was found to be 2× more potent than its (*S*)-binaphthyl analogue **74** (Table 5). Most notably, the addition of a second cationic amino acid residue conferred antimicrobial activity against Gram-negative bacteria to the Series **B** dicationic derivatives; compounds **70** and **71** exhibited MIC values ranging from 8–16 µg/mL against both *E. coli* and *P. aeruginosa* (Table 8). The general increase in antimicrobial activity seen with the addition of a second cationic residue is likely a result of the increased electrostatic interactions between the cationic molecule and the anionic bacterial membrane. Furthermore, an increase in the number of cationic residues relative to the hydrophobic substituents may confer a more optimized amphiphilic structure to the compounds. Compound **72** was found to exhibit the best MIC profile against Gram-positive bacteria amongst the Series **B** analogues.

2.2.3. Series C derivatives

The incorporation of a second bioisosteric 1,2,3-triazole moiety to give the Series **C** biphenyl dicationic terminal triazoles **78–85** resulted in a substantial increase in antibacterial efficacy against Gram-negative bacteria (Table 9). Compound **79** exhibited MIC values of 4–16 µg/mL against *P. aeruginosa*, *K. pneumoniae*, *A. baumannii* and *E.coli* (Table 9). The resultant increase in Gram-negative activity for the biphenyl bis-triazoles **78–85** was less easily explained, given that the same terminal bioisosteric 1,2,3-triazole substitution did not confer an increase in Gram-negative activity to the (*S*)-binaphthyl analogues **86** and **87**; these analogues exhibited similar Gram-negative MIC values relative to the Series **B** terminal amide analogues **70** and **71** (Tables 8 and 9). The balance of hydrophobicity and cationicity proved essential for effective antibacterial Gram-negative activity in compounds **78–85**; increasing the hydrophobicity (replacement of biphenyl with an (*S*)-binaphthyl, e.g. compounds **86** or **87** – Table 9) or decreasing the cationicity (e.g. Series **A** monocationic derivatives – Table 7) resulted in a loss of efficacy against Gram-negative bacteria. Compound **81** was identified as a potent derivative with broad spectrum activity, exhibiting MIC values of 2–4 µg/mL against all tested Gram-positive bacteria and 4–16 µg/mL against all tested Gram-negative bacteria.

2.2.4. Hydrophobic terminus variation

The presence of a terminal hydrophobic residue was essential for potent antimicrobial activity; compound **85**, which comprised a bare azide terminus rather than a 1,2,3-triazole linked hydrophobic residue, was found to exhibit MIC values that were 2–4× less potent than its related derivatives **82–84**. The essential nature of the hydrophobic terminus was also observed amongst the Series **A** monocationic derivatives, as hydrophilic termini (e.g. compounds **59** and **60**) resulted in decreased antibacterial efficacy (Table 4). For the Gram-positive bacteria, the more flexible, hydrophobic termini were found to be slightly more potent: e.g. compound **79** (phenethyl terminus) was slightly more potent than compound **78** (benzyl terminus) and compound **81** (cyclohexylmethyl terminus) was slightly more potent against some Gram-positive bacteria than compound **80** (cyclohexyl terminus) – see Table 6. This pattern was not observed amongst the Gram-negative bacterial species and no correlation between termini type and antibacterial activity could be drawn for the Gram-negative bacteria (Table 9).

2.2.4. Amino acid orientation

The orientation of the cationic residues was found to impact the antibacterial efficacy against specific strains. Reversing the Lys-Arg orientation (e.g. compounds **78–81**) to Arg-Lys (e.g. compounds **82–84**) did not drastically affect the MIC values against most bacterial species, although a substantial difference in antibacterial efficacy was observed for *C. difficile* and *K. pneumoniae*; the Lys-Arg orientation was found to be superior in both cases (Tables 6 and 9, respectively).

2.2.5. MIC testing against an extended panel of drug-resistant Gram-positive bacteria

Notably, MIC testing of compounds **45**, **49**, **71** and **73** against an extended panel of Gram-positive bacteria showed that the cationic amphiphiles exhibit potent antimicrobial activity against a broad range of drug-

resistant, Gram-positive pathogens (Table 10), including MRSA, vancomycin-resistant *S. aureus* (VRSA), vancomycin-resistant *E. faecalis* (VRE), MDR *S. pneumoniae* and *S. aureus* with reduced susceptibility to daptomycin. Potent MIC values of 1–4 µg/mL were observed for the dicationic amphiphiles **71** and **73** against every drug resistant Gram-positive bacteria tested. Antibacterial activity against these resistant isolates provides further evidence for a distinct mechanism of action relative to vancomycin, daptomycin and methicillin.

Table 4. Primary screening: antibacterial activities of Series **A** derivatives reported as MIC values (μg/mL).

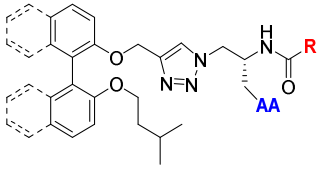

AA = Lys = 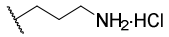

or

AA = Arg = 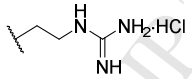

Entry	Compound	Aromatic Core	AA	R	*S. aureus* ATCC 29213	*S. aureus* NCTC 10442 (MRSA)	*E. faecalis* ATCC 29212	*S. pneumoniae* ATCC 49619	*C. difficile* ATCC 700057	*C. difficile* 132 (RT027)
1	**38**	Biphenyl	Lys	Bn	8	8	8	8	32	32
2	**39**	Biphenyl	Lys	PhEt	8	4	8	8	8	16
3	**40**	Biphenyl	Lys	OBn	16	16	16	32	8	32
4	**41**	Biphenyl	Arg	Bn	16	16	16	16	64	16
5	**42**	Biphenyl	Arg	PhEt	16	16	16	32	128	16
6	**43**	Biphenyl	Arg	OBn	4	4	8	16	32	32
7	**44**	(*S*)-Binaphthyl	Lys	Bn	8	8	8	32	16	32
8	**45**	(*S*)-Binaphthyl	Lys	PhEt	4	8	8	16	32	32
9	**46**	(*S*)-Binaphthyl	Lys	OBn	4	8	8	16	32	32
10	**47**	(*S*)-Binaphthyl	Lys	Ph	8	8	8	16	32	32
11	**48**	(*S*)-Binaphthyl	Lys	Phenylpropyl	8	16	8	32	32	64
12	**49**	(*S*)-Binaphthyl	Lys	Piperonyl	8	8	8	16	32	32
13	**50**	(*S*)-Binaphthyl	Lys	4-CH_3-Bn	8	8	8	32	16	32
14	**51**	(*S*)-Binaphthyl	Lys	Naphth-2-yl	16	16	8	32	64	64
15	**52**	(*S*)-Binaphthyl	Lys	4-Br-Bn	4	8	8	32	32	64
16	**53**	(*S*)-Binaphthyl	Lys	Furan-2-yl	8	8	8	16	16	32
17	**54**	(*S*)-Binaphthyl	Lys	Thiophen-2-yl	8	8	8	16	32	64
18	**55**	(*S*)-Binaphthyl	Lys	Cyclopentenyl	8	8	8	16	32	64
19	**56**	(*S*)-Binaphthyl	Lys	Cyclopropyl	8	8	8	16	16	64
20	**57**	(*S*)-Binaphthyl	Lys	Cyclohexenyl	8	8	8	16	32	32
21	**58**	(*S*)-Binaphthyl	Lys	Isobutyl	8	8	8	16	16	32
22	**59**	(*S*)-Binaphthyl	Lys	2-Pyrrolid-one-5-yl	16	16	16	32	32	64
23	**60**	(*S*)-Binaphthyl	Lys	4-NH_2-tetrahydropyran-4-yl	16	16	16	16	32	64
24	**61**	(*S*)-Binaphthyl	Arg	Bn	4	4	8	8	64	64
25	**62**	(*S*)-Binaphthyl	Arg	PhEt	4	4	8	8	16	16
26	**63**	(*S*)-Binaphthyl	Arg	OBn	4	4	8	8	32	32
27	Vancomycin	-	-	-	1	1	4	1	0.5	0.5

Table 5. Primary screening: antibacterial activities of Series **B** derivatives reported as MIC values (μg/mL).

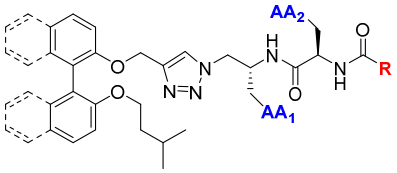

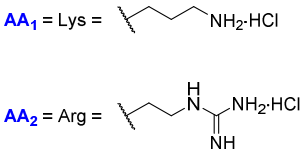

Entry	Compound	**Aromatic Core**	**R**	*S. aureus* ATCC 29213	*S. aureus* NCTC 10442 (MRSA)	*E. faecalis* ATCC 29212	*S. pneumoniae* ATCC 49619	*C. difficile* ATCC 700057	*C. difficile* 132 (RT027)
1	**68**	Biphenyl	Bn	8	8	8	8	16	16
2	**69**	Biphenyl	Fmo[a]	4	4	4	4	32	32
3	**70**	(*S*)-Binaphthyl	Bn	2	4	4	4	8	16
4	**71**	(*S*)-Binaphthyl	PhEt	4	4	4	4	16	32
5	**72**	(*S*)-Binaphthyl	Phenylpropyl	2	4	2	4	8	16
6	**73**	(*S*)-Binaphthyl	Piperonyl	4	4	4	4	8	32
7	**74**	(*S*)-Binaphthyl	Fmo[a]	8	8	8	8	32	64
8	Vancomycin	-	-	1	1	4	1	0.5	0.5

[a] Fluorenylmethyloxy (Fmo).

Table 6. Primary screening: antibacterial activities of Series **C** derivatives reported as MIC values (μg/mL).

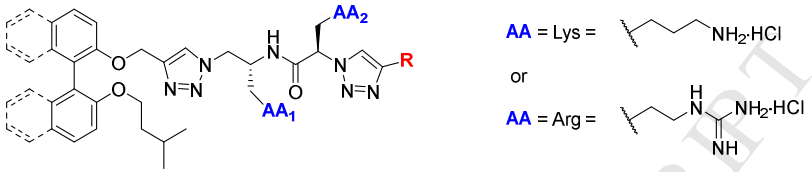

Entry	Compound	**Aromatic Core**	**AA_1**	**AA_2**	**R**	*S. aureus* ATCC 29213	*S. aureus* NCTC 10442 (MRSA)	*E. faecalis* ATCC 29212	*S. pneumoniae* ATCC 49619	*C. difficile* ATCC 700057	*C. difficile* 132 (RT027)
1	**78**	Biphenyl	Lys	Arg	Bn	8	8	16	4	16	16
2	**79**	Biphenyl	Lys	Arg	PhEt	4	4	8	8	8	8
3	**80**	Biphenyl	Lys	Arg	Cy	8	4	8	4	4	8
4	**81**	Biphenyl	Lys	Arg	CH_2Cy	4	4	4	4	4	4
5	**82**	Biphenyl	Arg	Lys	Bn	4	4	8	4	64	64
6	**83**	Biphenyl	Arg	Lys	PhEt	4	4	8	4	16	16
7	**84**	Biphenyl	Arg	Lys	Cy	4	4	8	4	32	32
8	**85**	Biphenyl	Arg	Lys	N/A[a]	16	16	16	8	64	32
9	**86**	(*S*)-Binaphthyl	Lys	Arg	PhEt	4	4	4	4	16	16
10	**87**	(*S*)-Binaphthyl	Lys	Arg	CH_2Cy	4	4	4	4	8	16
11	Vancomycin	-	-	-	-	1	1	4	1	0.5	0.5

[a] No terminal triazole moiety; synthesised by *N*-deprotection of the corresponding azide scaffold.

Table 7. Secondary screening: antibacterial activities of selected Series **A** derivatives reported as MIC values (μg/mL).

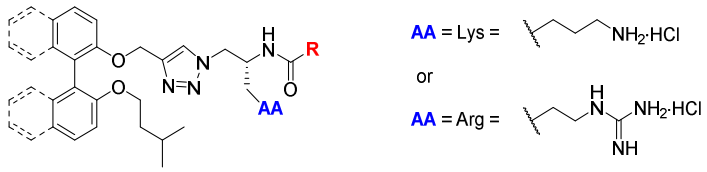

Entry	Compound	**Aromatic Core**	**AA**	**R**	*S. aureus* ATCC 43300 (MRSA)	*P. aeruginosa* ATCC 27853	*K. pneumoniae* ATCC 700603	*A. baumannii* ATCC 19606	*E. coli* ATCC 25922	Cytotoxicity (CC_{50}) (HEK-293) ATCC CRL-1573
1	**38**	Biphenyl	Lys	Bn	16	32	>32	32	>32	14.2
2	**39**	Biphenyl	Lys	PhEt	16	32	32	>32	32	4.8
3	**40**	Biphenyl	Lys	OBn	16	32	>32	32	32	4.7
4	**41**	Biphenyl	Arg	Bn	16	>32	>32	>32	>32	29.0
5	**42**	Biphenyl	Arg	PhEt	16	>32	>32	>32	>32	>32
6	**43**	Biphenyl	Arg	OBn	8	>32	>32	>32	>32	>32
7	**44**	(*S*)-Binaphthyl	Lys	Bn	8	>32	>32	>32	>32	8.6
8	**45**	(*S*)-Binaphthyl	Lys	OBn	4	>32	>32	>32	>32	3.5
9	**61**	(*S*)-Binaphthyl	Arg	Bn	4	>32	>32	>32	>32	16.5
10	**62**	(*S*)-Binaphthyl	Arg	PhEt	4	>32	>32	>32	>32	15.9
11	**63**	(*S*)-Binaphthyl	Arg	OBn	4	>32	>32	>32	>32	13.8
12	Vancomycin	-	-	-	1	-	-	-	-	-
13	Colistin	-	-	-	-	0.25	0.25	0.25	0.125	-
14	Tamoxifen	-	-	-	-	-	-	-	-	13.1

Table 8. Secondary screening: antibacterial activities of Series **B** derivatives reported as MIC values (μg/mL).

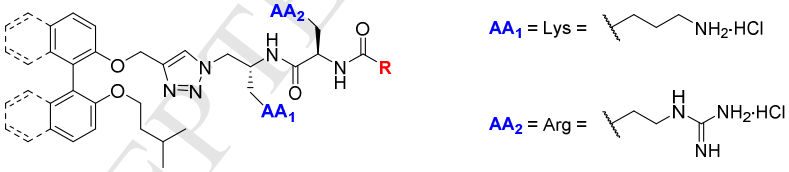

Entry	Compound	**Aromatic Core**	**R**	*S. aureus* ATCC 43300 (MRSA)	*P. aeruginosa* ATCC 27853	*K. pneumoniae* ATCC 700603	*A. baumannii* ATCC 19606	*E. coli* ATCC 25922	Cytotoxicity (CC_{50}) (HEK-293) ATCC CRL-1573
1	**68**	Biphenyl	Bn	4	32	32	32	16	32
2	**69**	Biphenyl	Fmo	4	>32	>32	>32	>32	>32
3	**70**	(*S*)-Binaphthyl	Bn	2	16	32	32	8	12.1
4	**71**	(*S*)-Binaphthyl	PhEt	2	16	32	32	8	27.4
5	Vancomycin	-	-	1	-	-	-	-	-
6	Colistin	-	-	-	0.25	0.25	0.25	0.125	-
7	Tamoxifen	-	-	-	-	-	-	-	13.1

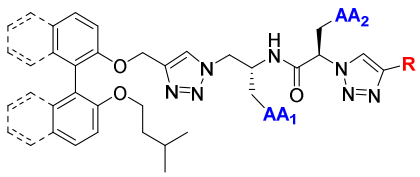

Entry	Compound	Aromatic Core	AA_1	AA_2	R	*S. aureus* ATCC 43300 (MRSA)	*P. aeruginosa* ATCC 27853	*K. pneumoniae* ATCC 700603	*A. baumannii* ATCC 19606	*E. coli* ATCC 25922	Cytotoxicity (CC_{50}) (HEK-293) ATCC CRL-1573
1	**78**	Biphenyl	Lys	Arg	Bn	4	16	16	8	16	21.9
2	**79**	Biphenyl	Lys	Arg	PhEt	2	8	16	16	8	>32
3	**80**	Biphenyl	Lys	Arg	Cy	4	8	16	16	8	14.2
4	**81**	Biphenyl	Lys	Arg	CH_2Cy	2	16	16	8	4	>32
5	**82**	Biphenyl	Arg	Lys	Bn	4	16	32	16	8	17.8
6	**83**	Biphenyl	Arg	Lys	PhEt	2	8	16	16	4	17.4
7	**84**	Biphenyl	Arg	Lys	Cy	4	8	32	8	8	15.3
8	**85**	Biphenyl	Arg	Lys	N/A[a]	8	32	32	16	16	>32
9	**86**	(*S*)-Binaphthyl	Lys	Arg	PhEt	4	32	>32	32	>32	>32
10	**87**	(*S*)-Binaphthyl	Lys	Arg	CH_2Cy	2	32	>32	16	32	>32
11	Vancomycin	-	-	-	-	1	-	-	-	-	-
12	Colistin	-	-	-	-	-	0.25	0.25	0.25	0.125	-
13	Tamoxifen	-	-	-	-	-	-	-	-	-	13.1

Table 9. Secondary screening: antibacterial activities of selected Series **C** derivatives, reported as MIC values (μg/mL).

[a] No terminal triazole moiety; synthesised by *N*-deprotection of the corresponding azide scaffold.

Table 10. Extended Gram-positive screening panel: antibacterial activities of selected derivatives, reported as MIC values (μg/mL).

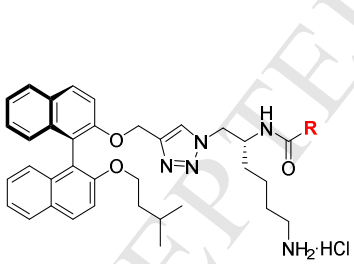

45 and **49**

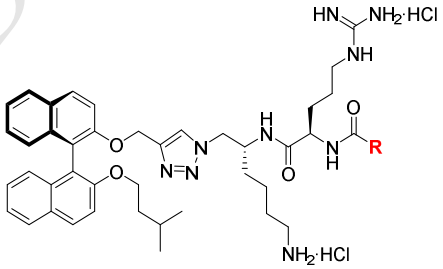

71 and **73**

Entry	Compound	R	*S. aureus* ATCC 43300 (MRSA)	*S. aureus* clinical isolate (MRSA)	*S. aureus* NRS17 (GISA)[a]	*S. aureus* NRS1 (GISA/ MRSA)	*S. aureus* clinical isolate (MRSA)[b]	*S. aureus* VRS10 – (VRSA)[c]	*S. pneumoniae* ATCC700677 (MDR)	*E. faecalis* clinical isolate (VRE)
1	**45**	OBn	2-4	16	8	8-16	8	8	8	4
2	**49**	Piperonyl	8	>32	16	8-16	8	8-16	8-16	4
3	**71**	PhEt	1-2	4	2	2-4	2-4	2	1-2	2
4	**73**	Piperonyl	2	4	4	2-4	4	4	2	2
5	Vancomycin	-	1	2	8	8	2	2	1-2	>32
6	Daptomycin	-	0.5-1	2	8	8	4	2	1-2	8

[a] Glycopeptide intermediate susceptibility *S. aureus* (GISA)
[b] MRSA/reduced daptomycin susceptibility
[c] Vancomycin resistant *S. aureus* (VRSA)
[d] Vancomycin resistant *E. faecalis* (VRE)

2.3. Haemolysis Assay

To determine the membrane selectivity of the biaryl cationic peptidomimetics, selected derivatives were subjected to a haemolysis assay with sheep erythrocytes at concentrations of 5 µg/mL and 50 µg/mL; UltraPure H_2O was utilized as a positive control (i.e. 100% haemolysis) and the results are displayed in Table 11.

Table 11. Percent haemolysis assay for selected derivatives from Series **A**, **B** and **C**.

Entry	Compound	Testing Concentration	
		5 µg/mL	50 µg/mL
1	**39**	0.2%	100.8%
2	**43**	0.7%	89.1%
3	**61**	1.0%	87.4%
4	**68**	0.6%	17.5%
5	**71**	1.1%	94.2%
6	**80**	1.9%	22.9%
7	**81**	1.5%	42.4%
8	**83**	1.7%	28.8%
9	**87**	1.6%	88.8%

All compounds tested exhibited minimal haemolysis at the lower testing concentration of 5 µg/mL. The Series **A** monocationic derivatives **39**, **43** and **61** displayed strong haemolysis at the higher concentration of 50 µg/mL; these compounds displayed minimal membrane selectivity, effectively disrupting mammalian membranes at higher concentrations. The biphenyl dicationics **68**, **80**, **81** and **83** all exhibited <50% haemolysis at 50 µg/mL, while the (*S*)-binaphthyl dicationic analogues **71** and **87** displayed 94.2% and 88.8% haemolysis, respectively, at this higher testing concentration. The biphenyl dicationic derivatives exhibited lower haemolysis; their optimized cationic/hydrophobic ratio conferred increased membrane selectivity and therefore, reduced haemolysis. The increased hydrophobicity of the (*S*)-binaphthyl dicationic analogues **71** and **87** resulted in increased haemolysis, due to a decrease in the cationic/hydrophobic ratio relative to compounds **68**, **80**, **81** and **83**. This correlation between the cationic/hydrophobic ratio and membrane selectivity will benefit the rational design of future amphiphilic AMP mimics.

2.4. Time kill kinetics assay

Compound **71** was selected for an *in vitro* time-kill assay against *S. aureus* (ATCC 29213) and *E. coli* (ATCC 25922) to ascertain the bactericidal kinetics of the cationic amphiphilic peptidomimetics synthesized in this study. A testing concentration of 64 µg/mL (16 × MIC for *S. aureus* and 8 × MIC for *E. coli*) was utilized and the results indicated that compound **71** killed *S. aureus* in ≤30 min and *E. coli* in ≤120 min (i.e. a ≥3-$\log_{10}$ reduction in bacteria - see Fig. 3). After 6 h, vancomycin displayed only a minimal reduction in *S. aureus* viability (Fig. 3, top), suggesting a distinct mode of action relative to the fast-acting cationic amphiphiles (e.g. compound **71**). After 2 h, colistin reduced the *E. coli* loading below the limit of detection (Fig. 3, bottom), similar to compound **71**. Colistin is known to cause membrane-disruption of Gram-negative bacteria [9]; the comparable fast-acting bactericidal kinetics of compound **71** are congruent with gross membrane-disruption.

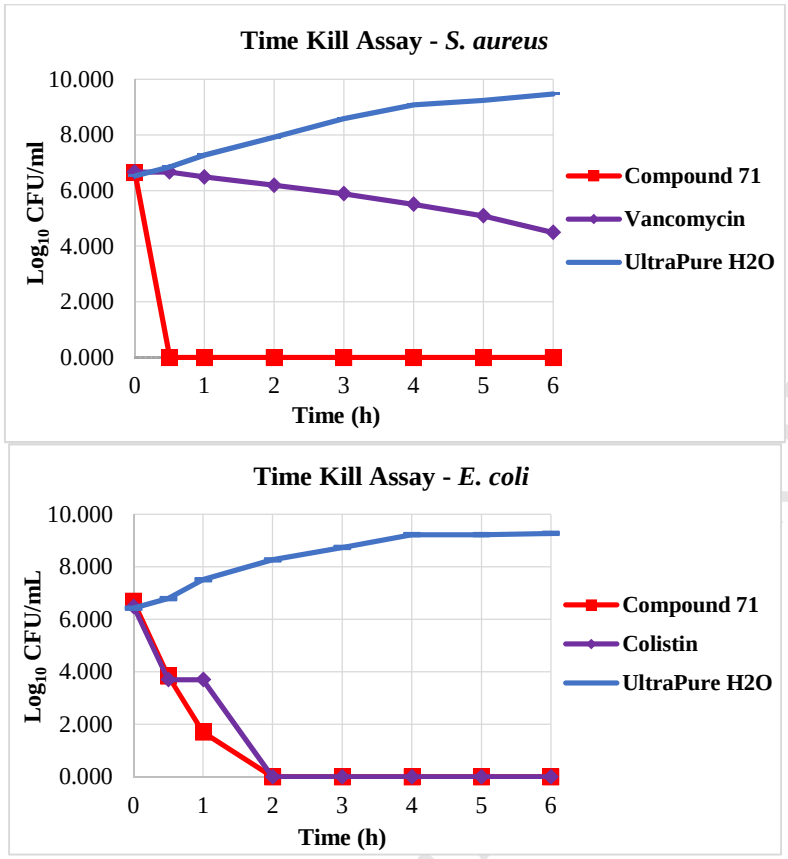

Fig. 3. Time kill assays for compound **71** at 64 µg/mL against *S. aureus* (top) and *E. coli* (bottom). Limit of detection = 10^3 CFU/mL. Vancomycin tested at 8 µg/mL (8 × MIC) and colistin tested at 4 µg/mL (32 × MIC).

2.5. Cytoplasmic membrane depolarization assay

A cytoplasmic membrane depolarization assay with 3,3′-dipropylthiadicarbocyanine ($diSC_3(5)$) fluorescent dye [13, 17] was performed on compounds **39**, **71** and **81** against *S. aureus* and *E. coli* to investigate the mode of action for these cationic amphiphilic peptidomimetics. The electrochemical membrane potential forces the cationic $diSC_3(5)$ dye to sequester into the bilayer lipid membrane of the bacteria, thereby quenching its own fluorescence; when the cytoplasmic membrane potential is disrupted by the antimicrobial compounds, the $diSC_3(5)$ dye leaks out and causes an observable increase in fluorescence.

Compounds **39**, **71** and **81** were found to strongly disrupt the membrane potential of *S. aureus* (ATCC 29213) and *E. coli* (NCTC 10418) when tested at 32 and 64 µg/mL, respectively (i.e. 4–32 × MIC). For *S. aureus*, the fluorescence intensity increased by approximately 120–180% after exposure to the peptidomimetic compounds (Fig. 4, top). DMSO (20% aq.) was utilized as positive control and it resulted in a 90% increase in the observed fluorescence. Vancomycin and UltraPure H_2O were utilized as negative controls; as expected, both controls failed to generate any increase in fluorescence, further confirming the lack of membrane disruption for vancomycin. In the assay against *E. coli*, the fluorescence intensity increased by approximately 460–900% after exposure to the peptidomimetics (Fig. 4, bottom). DMSO (20% aq. – positive control) also exhibited a 900% increase in observed fluorescence against *E. coli*, whereas colistin (positive control for *E. coli*) displayed an approximate 400% increase in the observed fluorescence. The bis-triazole compound **81** exhibited the lowest MIC values (i.e. 2 µg/mL for MRSA and 4 µg/mL for *E. coli*) out of the three compounds subjected to cytoplasmic membrane depolarization assay and it was also found to exhibit the highest fluorescence in the assay against both *S. aureus* and *E. coli*. These results indicate a positive correlation between membrane depolarization activity and antibacterial efficacy, as would be expected for membrane-active antibacterial compounds.

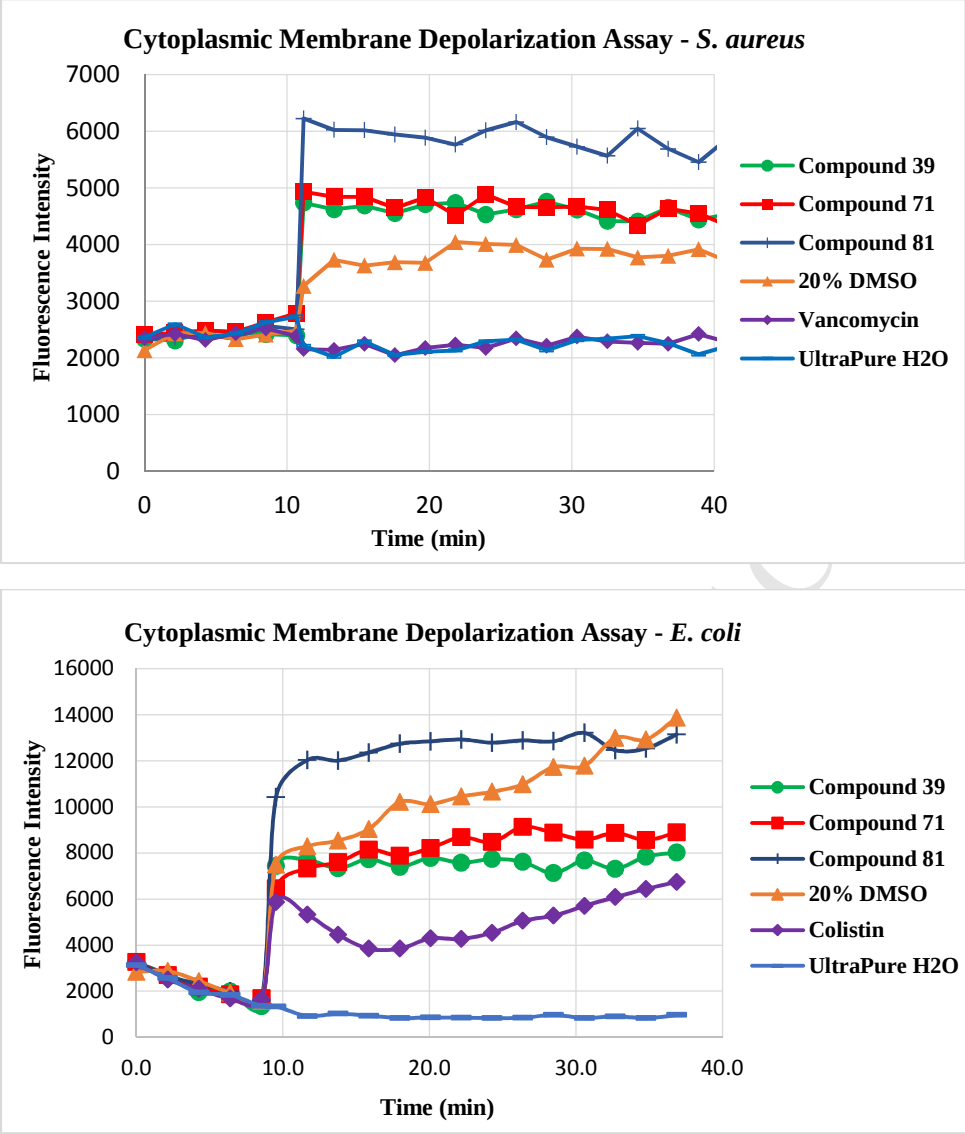

Fig. 4. Cytoplasmic membrane depolarization assays for compounds **39**, **71** and **81** tested at 32 µg/mL against *S. aureus* (top) and 64 µg/mL against *E. coli* (bottom). Vancomycin tested at 8 µg/mL and colistin tested at 64 µg/mL.

2.6. Cytoplasmic membrane permeabilization assay

A cytoplasmic membrane permeabilization assay with propidium iodide [17-18] was performed on compounds **39**, **71** and **81** against *S. aureus* (ATCC 29213) and *E. coli* (NCTC 10418) to confirm their membrane-disrupting ability. The propidium iodide dye does not permeate the cellular membrane of the bacteria unless the membrane has been disturbed; if large enough pores are formed, the dye can enter the cytoplasm and stain the DNA, which results in fluorescence.

The tested compounds (**39**, **71** and **81**) were found to effectively permeabilize the cytoplasmic membrane of *S. aureus* (Fig. 5, top). A 600% increase in fluorescence was observed for the tested compounds, indicating that the dye had permeated the cellular membrane of the bacteria. As expected, both vancomycin and UltraPure H_2O failed to give an increase in fluorescence. Interestingly, the fluorescence did not correlate with the MIC values, as the least potent monocationic derivative **39** gave the strongest fluorescence and the most potent compound **81** gave the weakest fluorescence. The dicationic derivatives (**71** and **81**) took much longer (~30 min) to reach a maximum fluorescence, relative to the monocationic derivative **39** (<10 min); these results indicate that the smaller, monocationic derivatives can permeabilize the cellular membrane more rapidly than the larger, dicationic derivatives. The monocationic compound **39** displayed a 75% increase in the observed fluorescence when tested against *E. coli*, similar to the positive control, colistin (Fig. 5, bottom), indicating successful permeabilization of the cellular membrane. The dicationic analogues **71** and **81** exhibited much lower levels of

increased fluorescence (25–40%), demonstrating a decreased propensity for permeabilization of Gram-negative cellular membranes relative to the monocationic analogue **39**.

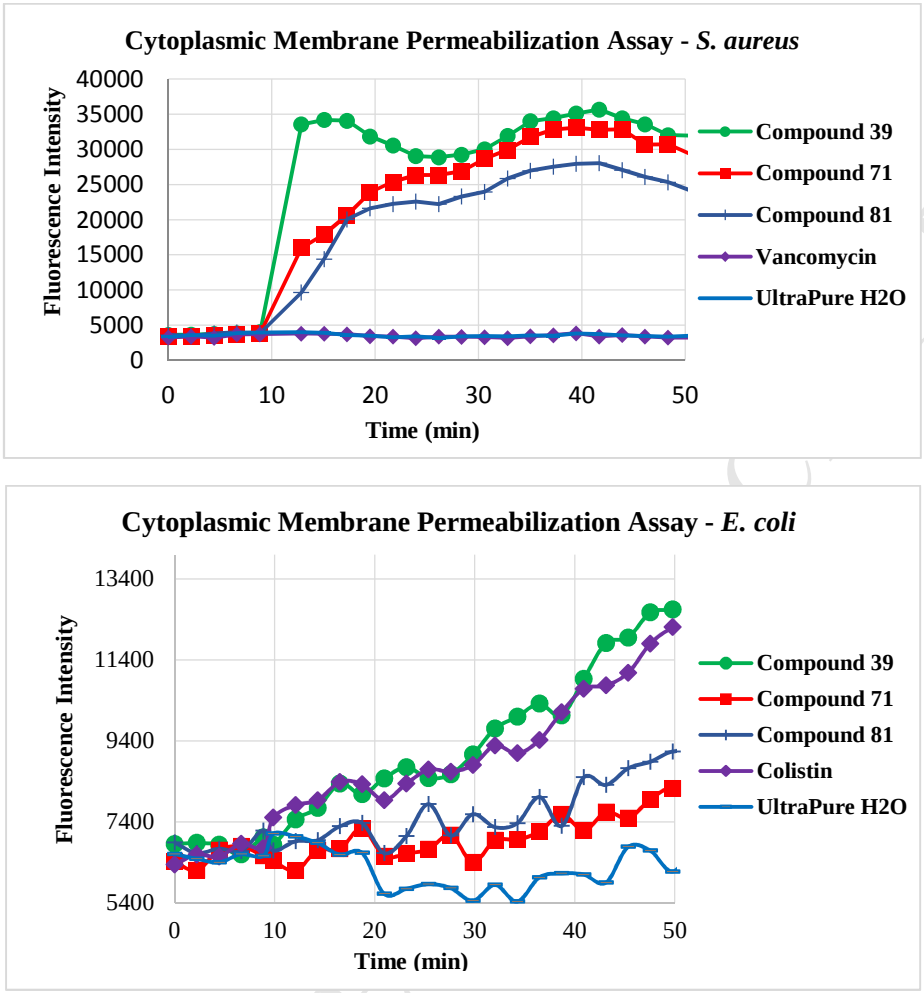

Fig. 5. Cytoplasmic membrane permeabilization assays for compounds **39**, **71** and **81** tested at 32 µg/mL against *S. aureus* (top) and *E. coli* (bottom). Vancomycin tested at 8 µg/mL and colistin tested at 64 µg/mL.

3. Conclusion

In total, forty-three cationic biaryl 1,2,3-triazolyl amphiphilic peptidomimetics were designed and prepared for antibacterial evaluation, including twenty-six monocationic amide analogues (**A**), seven dicationic amide analogues (**B**) and ten dicationic bis-triazole analogues (**C**). *In vitro* antibacterial susceptibility assays revealed that the synthesized 1,2,3-triazolyl amphiphiles maintained significant antimicrobial efficacy relative to the prototypical lead compound **1**. The dicationic bis-triazole derivatives (Series **C**) were found to exhibit potent antibacterial activity, with compound **81** displaying MIC values of 2–4 µg/mL against all Gram-positive bacteria tested and 4–16 µg/mL against all Gram-negative bacteria tested. Compound **81** also showed increased Gram-negative efficacy, relative to the monocationic and dicationic amide analogues (Series **A** and **B**, respectively) which displayed reduced or no antibacterial activity against the tested Gram-negative pathogens. Furthermore, the synthesized peptidomimetics were shown to exhibit excellent *in vitro* activity against multiple drug resistant Gram-positive strains, including MRSA, VRSA, VRE and *S. aureus* with reduced susceptibility to daptomycin.

The ratio of cationic/hydrophobic moieties within the peptidomimetic amphiphiles was found to have a strong influence on their antimicrobial activity, haemolytic activity and membrane selectivity. The dicationic biphenyl bis-triazole derivatives (e.g. compound **81**) were found to exhibit strong Gram-negative activity, but the corresponding (*S*)-binaphthyl analogues and monocationic derivatives were lacking sufficient activity against Gram-negative bacteria, likely due to steric bulk and/or a suboptimal amphiphilic conformation. The monocationic derivatives (Series **A**) were notably haemolytic due to a non-optimized amphiphilic structure; the

addition of a second cationic residue (to give Series **B** and **C**) conferred a more ideal amphiphilic conformation due to the cationic/hydrophobic ratio, thus resulting in increased antimicrobial activity and reduced haemolytic activity relative to the monocationic derivatives. Further optimization of the haemolytic activity and membrane selectivity will be necessary before this class of compounds can be considered for systemic application.

Cytoplasmic membrane depolarization and permeabilization assays provided evidence of a membrane-active mechanism; compounds **39**, **71** and **81** were found to strongly disrupt the membrane potential and permeabilize the cellular membrane of both *S. aureus* and *E. coli*. A time-kill kinetics assay further confirmed the likely mode of action, as compound **71** exhibited extremely rapid antibacterial efficacy, killing *S. aureus* within 30 min and *E. coli* within 2 h; these rapid bactericidal kinetics are similar to those of other membrane-active molecules (e.g. colistin).

These preliminary investigations have revealed a likely mode of action for the 1,2,3-triazolyl biarylpeptidomimetics and they have provided further insight into the structural elements influencing the antimicrobial efficacy and haemolytic activity of the synthesized peptidomimetics.

4. Experimental section

4.1. General information

Synthesis

Unless stated otherwise, all solvents and chemicals were laboratory or reagent grade and were purchased from commercial sources. All chemicals were used as received. Water was purified *via* Millipore filtration prior to use. HOBt and propargyl bromide were purchased with added stabilizers (10% w/w H_2O and 20% w/w toluene, respectively); therefore, the quantities required for reactions were adjusted accordingly and are reflected in the reagent masses reported in the experimental (whereas the reported mmol quantities reflect the true quantity of chemical). All reactions were conducted under normal atmosphere and cold reaction temperatures were obtained by an ice bath (0 ºC) or ice/salt bath (–10 ºC). Heating of reactions was performed with a paraffin oil bath. Small quantities of liquid reagents were measured and added to reactions *via* syringe or autopipette. Unless otherwise noted, all filtrations were conducted as vacuum filtration through a sintered glass funnel (medium porosity). Vacuum filtration was achieved with the aid of a water aspirator. Solvent removal *via* concentration was performed on a rotary evaporator under reduced pressure. All solvent mixtures are expressed in terms of volume ratio (i.e. v/v). Thin layer chromatography (TLC) was performed on aluminium-backed SiO_2 gel plates (F_{254} grade - 0.20 mm thickness). Visualization was achieved with UV light, ninhydrin stain or cerium ammonium molybdate stain. Flash chromatography was performed on SiO_2 gel 60 with positive air pressure. All synthesized compounds were dried under high vacuum (<1 mbar) before determination of chemical yields and spectroscopic characterization.

Characterization and analysis

^{1}H NMR spectra were recorded on a Bruker Avance 400 (400 MHz), a Varian VNMRS PS54 500 (500 MHz), a Varian Inova 500 (500 MHz) or a Varian Mercury 300 (300 MHz) NMR spectrometer. Chemical shifts are reported in ppm and were measured relative to the internal standard. Samples were dissolved in $CDCl_3$ (with TMS as the internal standard – 0.00 ppm), CD_3OD (solvent resonance as internal standard – 3.31 ppm) or DMSO-d_6 (solvent resonance as internal standard – 2.50 ppm). The ^{1}H NMR data is reported as follows: chemical shift, multiplicity (s = singlet, d = doublet, t = triplet, q = quartet, dt = doublet of triplets, m = multiplet, br = broad), coupling constants (Hz) and integration. ^{13}C NMR spectra were recorded on a Bruker Avance 400 (101 MHz), a Varian VNMRS PS54 500 (126 MHz), a Varian Inova 500 (126 MHz) or a Varian Mercury 300 (75 MHz) NMR spectrometer with complete ^{1}H decoupling. Chemical shifts are reported in ppm and were measured relative to the internal standard. Samples were dissolved in $CDCl_3$ (solvent resonance as the internal standard – 77.16 ppm), CD_3OD (solvent resonance as the internal standard – 49.20 ppm) or DMSO-d_6 (solvent resonance as internal standard – 39.50 ppm). Variable temperature NMR experiments were performed at 90 °C on the Bruker Avance 400 NMR spectrometer. ^{1}H and ^{13}C NMR assignments were confirmed by analysis of NMR APT, gCOSY, gHSQC, gHMBC and/or zTOCSY experiments. Ambiguous degenerate carbon resonances are marked with a single asterisk * (representing two carbons) or a double asterisk ** (representing three or more carbons) for clarity. Carbon resonances that required 2-D NMR analysis for assignment (i.e. not

observed *via* 1-D ^{13}C NMR analysis) are marked with the label "*observed by gHMBC*" or "*observed by gHSQC*". NMR spectra were processed, analysed and prepared with MestReNova (version 6.0) NMR software. Low-resolution mass spectra (LRMS) were obtained *via* electrospray ionization (ESI) on a Shimadzu LC-2010 mass spectrometer. LRMS data was recorded as the ion mass/charge ratio (*m*/*z*) with the corresponding relative abundance as a percentage. High-resolution mass spectrometry (HRMS) was performed on a Waters Quadrupole-Time of Flight (QTOF) Xevo spectrometer *via* ESI and with Leucine-Enkephalin as an internal standard. All mass spectrometry samples were dissolved in high-performance liquid chromatography (HPLC) grade MeOH (containing <1% formic acid for ionization). Optical rotations were measured on a Jasco P-2000 polarimeter with a 10 cm path length; rotation values (α) are expressed in units of "deg cm^3 g^{-1} dm^{-1}" with concentration (*c*) expressed in units of "g/100 mL". Solid-state infrared spectroscopy was performed on a Shimadzu IRAffinity-1 FTIR spectrometer in combination with a MIRacle 10 Single Reflection Attenuated Total Reflectance accessory outfitted with a 1.5 mm round diamond crystal. IR peaks are reported as the wavenumber ($\overline{\nu}_{max}$ in cm^{-1}) of the maximum absorption. Analytical HPLC was performed on a Phenomenex Synergi 4u Fusion-Reverse Phase 80Å column (ϕ = 4.6 × 150 mm) with detection at λ = 215 nm and H_2O/CH_3CN (both containing 0.1% TFA) as the mobile phase.

Notes and other considerations

Known reagents that were not available commercially were prepared according to the literature procedures cited within the supplementary information. The experimental section contains a representative synthesis of final compound **81** utilizing the general synthetic procedures outlined in Section 4.2; the synthetic and characterization data for all other compounds can be found within the supplementary information. Synthesized compounds that contain the (*S*)-isopentyloxy-binaphthalene fragment and some chiral compounds that contain the isopentyloxybiphenyl fragment exhibited a pair of diastereotopic methyl (-CH_3) groups on the terminus of the isopentyl substituent; these carbons are consistently referred to as C4″ and C5″. Importantly, these two carbons (and associated protons) would sometimes exhibit distinct chemical shifts due to the chiral environment imposed by the amino acid residue(s) (for all derivatives) and/or the adjacent (*S*)-binaphthyl moiety (for (*S*)-binaphthyl derivatives only).

4.2. General synthetic procedures

General Procedure A: Copper catalyzed azide-alkyne cycloaddition

To a reaction vessel charged with the azide (1.0 eq), alkyne (2.0 – 3.0 eq), $Cu(OAc)_2 \cdot H_2O$ (0.2 eq), and sodium ascorbate (0.4 eq) was added *t*-BuOH (20 mL/mmol azide) and H_2O (5 mL/mmol azide). The mixture was initially sonicated for < 1 min followed by vigorous stirring at rt (unless noted otherwise) for the specified time. The reaction mixture was diluted with EtOAc (20 mL for reactions that contained ≤ 1.0 mmol azide or 20 mL/mmol azide for larger scale reactions) and washed with an equivalent volume of saturated aqueous NH_4Cl solution (e.g. 20 mL). The organic phase was dried ($MgSO_4$), filtered, concentrated and the residue was subjected to flash chromatography over SiO_2 gel to afford the desired 1,4-disubstituted-1,2,3-triazole product.

General Procedure B: Amide coupling

The amine (1.0 eq), carboxylic acid (1.0 – 1.2 eq), EDCI (1.2 eq) and HOBt (1.1 eq) were combined in an acetonitrile solution (10 mL/mmol amine) and stirred at rt for the specified time. The solvent was removed (not required for ≤ 5.0 mL acetonitrile) and the residue was dissolved in EtOAc (25 mL for reactions that contained ≤ 1.0 mmol amine or 25 mL/mmol amine for larger scale reactions). The organic solution was washed successively with aqueous HCl (1.0 M – 2 × 25 mL), saturated aqueous $NaHCO_3$ (3 × 25 mL) and brine (1 × 25 mL). The EtOAc solution was dried ($MgSO_4$), filtered and concentrated. If necessary, the residue was subjected to further purification *via* flash chromatography over SiO_2 gel to furnish the targeted amide product.

General Procedure C: Amine deprotection (N-Boc and/or N-Pbf removal)

The *N*-protected amine (1.0 eq) was dissolved in a CH_2Cl_2 (30 mL/mmol substrate) with magnetic stirring. If the substrate molecule contained an *N*-Pbf moiety then H_2O (20.0 eq) was also added to the solution. TFA (30.0 mL/mmol substrate) was then added and the reaction mixture was stirred at rt overnight (> 16 h) followed by removal of the solvent. The residue was dissolved in CH_2Cl_2 (30 mL/mmol substrate), an excess amount of

anhydrous HCl (2.0 M in Et_2O, 15 mL/mmol substrate, 30.0 eq) was added and the solvent was then removed. The resulting residue was dissolved in a minimal volume of CH_2Cl_2 (or MeOH) and excess Et_2O (25 mL for ≤ 0.1 mmol substrate) was added to precipitate the hydrochloride salt of the amine. The solvent was removed by filtration and the product (both in the filter funnel and in the flask) was triturated with Et_2O (3 × 20 mL). The product was collected by dissolution in MeOH; concentration followed by drying *in vacuo* gave the final mono- or di-hydrochloride salt as a thin, translucent film that was routinely scratched with a spatula into a fine hygroscopic powder or amorphous gum.

General Procedure D: Modified amine deprotection (N-Boc removal)

For the biphenyl monocationic lysine derivatives (**38–40**), **General Procedure C** was followed with the following modifications: Et_2O (instead of CH_2Cl_2 or MeOH) was utilized to dissolve the residue for final precipitation and petroleum ether (P.E. – instead of Et_2O) was utilized as the antisolvent for precipitation.

4.3. Representative synthesis of compound **81** *from precursor building blocks* **15** *and* **21**

*4.3.1. Benzyl ((R)-N^6-(tert-butoxycarbonyl)-6-amino-1-(4-(((2'-(isopentyloxy)-[1,1'-biphenyl]-2-yl)oxy)methyl)-1H-1,2,3-triazol-1-yl)hexan-2-yl)carbamate (**29**)*

Following **General Procedure A**, azide **21** (1.50 g, 3.83 mmol), alkyne **15** (2.26 g, 7.66 mmol), $Cu(OAc)_2{\cdot}H_2O$ (153 mg, 0.77 mmol) and sodium ascorbate (304 mg, 1.53 mmol) were stirred in *t*-BuOH (77 mL) and H_2O (19 mL) for 48 h to give the triazole **29** (1.97 g, 75%) as a white foam after flash chromatography over SiO_2 gel (EtOAc/P.E. – 20:80 → 50:50). TLC (EtOAc/P.E. – 50:50): R_f = 0.48; $[\alpha]_D^{23}$ +31.3 (*c* 0.83, MeOH); ^{1}H NMR (400 MHz, $CDCl_3$) δ 7.38 – 7.21 (m, 9H), 7.17 (s, 1H), 7.07 – 6.99 (m, 2H), 6.99 – 6.91 (m, 2H), 5.14 (s, 2H), 5.06 (s, 3H), 4.55 (br s, 1H), 4.39 (d, *J* = 5.1 Hz, 2H), 3.92 (br s, 1H), 3.88 (t, *J* = 6.6 Hz, 2H), 3.06 (br s, 2H), 1.62 – 1.52 (m, 1H), 1.52 – 1.23 (m, 17H), 0.79 (d, *J* = 6.6 Hz, 6H); ^{13}C NMR (101 MHz, $CDCl_3$) δ 156.6, 156.2, 155.9, 155.8, 145.2, 136.2, 131.7, 131.5, 128.7, 128.54*, 128.46, 128.2, 128.1*, 123.3, 121.1, 120.1, 113.3, 112.3, 79.2, 67.0, 66.9, 63.4, 53.1, 51.2, 39.8, 37.9, 31.0, 29.7, 28.4, 25.0, 22.7, 22.5*; IR (neat) $\bar{\nu}_{max}$ 3323, 2952, 2930, 2869, 2358, 2342, 1696, 1506, 1437, 1394, 1364, 1242, 1166, 1052, 1011, 856, 750, 697 cm^{-1}; MS (ESI +ve) *m/z* 708 ($[M + Na]^+$, 100%), 686 ($[M + H]^+$, 22%); HRMS (ESI +ve TOF) calcd for $C_{39}H_{51}N_5O_6Na$ 708.3737, found 708.3755 ($[M + Na]^+$).

*4.3.2. Tert-butyl (R)-(5-amino-6-(4-(((2'-(isopentyloxy)-[1,1'-biphenyl]-2-yl)oxy)methyl)-1H-1,2,3-triazol-1-yl)hexyl)carbamate (**34**)*

To a reaction vessel charged with carbamate **29** (1.90 g, 2.77 mmol), acetic acid (3.17 mL, 55.40 mmol) and palladium on charcoal (10% w/w – 442 mg, 0.42 mmol) was added MeOH (27.7 mL) under a flow of N_2 gas. The reaction vessel was then sealed and degassed under high vacuum with magnetic stirring. N_2 gas was allowed into the reaction vessel and the vessel was again degassed; this step was done twice. After the third degassing, the vacuum was maintained and a 2.0 L balloon of H_2 gas was attached and allowed into the reaction vessel. The reaction mixture was then stirred vigorously at rt for 24 h under an atmosphere of H_2 gas. After the reaction was shown to be complete by TLC analysis (EtOAc/P.E. – 50:50), the H_2 source was removed, the reaction vessel was purged with N_2 gas and Celite was added to the reaction mixture with vigorous magnetic stirring. The mixture was then vacuum filtered through a pad of fresh Celite atop a PTFE membrane, the solids were rinsed thoroughly with MeOH (5 × 20 mL) and the combined filtrates were concentrated until nearly dry. The residue was dissolved in CH_2Cl_2 (200 mL) and washed successively with saturated aqueous $NaHCO_3$ (3 × 100 mL), H_2O (1 × 100 mL) and finally brine (1 × 100 mL). The organic phase was dried (Na_2SO_4), filtered and concentrated to afford the amine **34** (1.52 g, 99%) as translucent, light tan gum. TLC (NEt_3/MeOH/CH_2Cl_2 – 2:10:88): R_f = 0.46; $[\alpha]_D^{23}$ +16.5 (*c* 1.67, MeOH); ^{1}H NMR (400 MHz, $CDCl_3$) δ 7.34 – 7.22 (m, 5H), 7.08 – 6.92 (m, 4H), 5.17 (d, *J* = 0.8 Hz, 2H), 4.57 (br s, 1H), 4.28 (dd, *J* = 13.6, 4.2 Hz, 1H), 4.07 (dd, *J* = 13.6, 7.9 Hz, 1H), 3.90 (t, *J* = 6.6 Hz, 2H), 3.21 – 3.02 (m, 3H), 1.68 – 1.21 (m, 18H), 0.80 (d, *J* = 6.6 Hz, 6H); ^{13}C NMR (101 MHz, $CDCl_3$) δ 156.6, 156.0, 155.8, 145.2, 131.62, 131.56, 128.7, 128.50, 128.49, 128.2, 123.1, 121.1, 120.1, 113.2, 112.3, 79.2, 67.1, 63.54, 57.0, 51.5, 40.2, 38.0, 34.5, 30.0, 28.5, 25.0, 23.0, 22.5*; IR (neat) $\bar{\nu}_{max}$ 3345, 2955, 2930, 2869, 2362, 2327, 1700, 1506, 1437, 1388, 1364, 1241, 1166, 1125, 1051, 1002, 852, 750, 615 cm^{-1}; MS (ESI +ve) *m/z* 574 ($[M + Na]^+$, 100%), 552 ($[M + H]^+$, 80%); HRMS (ESI +ve TOF) calcd for $C_{31}H_{46}N_5O_4$ 552.3550, found 552.3564 ($[M + H]^+$).

*4.3.3. Tert-butyl ((R)-5-((R)-2-azido-5-(2-((2,2,4,6,7-pentamethyl-2,3-dihydrobenzofuran-5-yl)sulfonyl)guanidino)pentanamido)-6-(4-(((2'-(isopentyloxy)-[1,1'-biphenyl]-2-yl)oxy)methyl)-1H-1,2,3-triazol-1-yl)hexyl)carbamate (**75**)*

Following **General Procedure B**, amine **34** (300 mg, 0.54 mmol), acid **26** (271 mg, 0.60 mmol), EDCI (125 mg, 0.65 mmol) and HOBt (88 mg, 0.60 mmol) were stirred in acetonitrile (5.4 mL) for 48 h to give the amide **75** (479 mg, 89%) as a translucent tan gum after flash chromatography over SiO_2 gel (EtOAc/P.E. – 30:70 → 80:20). TLC (EtOAc/P.E. – 80:20): R_f = 0.53; $[\alpha]_D^{23}$ −14.7 (*c* 2.97, MeOH); ^{1}H NMR (400 MHz, $CDCl_3$) δ 7.48 (br s, 2H), 7.33 – 7.19 (m, 4H), 7.09 (d, *J* = 8.0 Hz, 1H), 7.05 – 6.92 (m, 3H), 6.26 (br s, 2H), 5.90 (br s, 1H), 5.11 (s, 2H), 4.70 (br s, 1H), 4.49 – 4.32 (m, 3H), 3.97 – 3.82 (m, 3H), 3.35 (br s, 1H), 3.06 (br s, 2H), 2.95 (s, 2H), 2.89 (br s, 1H), 2.58 (s, 3H), 2.51 (s, 3H), 2.09 (s, 3H), 1.63 – 1.19 (m, 28H), 0.80 (d, *J* = 6.5 Hz, 6H); ^{13}C NMR (101 MHz, $CDCl_3$) δ 170.9, 159.0, 156.5, 156.4, 156.3, 156.1, 144.6, 138.4, 132.7, 132.3, 131.9, 131.8, 128.9, 128.4, 128.0, 124.8, 124.0, 121.5, 120.5, 117.7, 114.2, 112.8, 86.6, 79.2, 67.3, 63.7, 61.0, 53.7, 49.4, 43.4, 40.3, 38.5, 38.0, 31.6, 29.6, 28.7, 28.5, 27.6, 25.6, 25.1, 23.1, 22.6, 22.5, 19.5, 18.1, 12.6; IR (neat) $\bar{\nu}_{max}$ 3455, 3335, 2954, 2933, 2875, 2375, 2331, 2104, 1689, 1653, 1559, 1540, 1512, 1457, 1437, 1368, 1243, 1162, 1107, 1091, 1053, 1031, 1003, 903, 853, 807, 784, 751, 734, 663, 641, 617 cm^{-1}; MS (ESI +ve) *m/z* 1009 ([M + Na]$^+$, 100%), 987 ([M + H]$^+$, 17%); HRMS (ESI +ve TOF) calcd for $C_{50}H_{72}N_{11}O_8S$ 986.5286, found 986.5305 ([M + H]$^+$).

*4.3.4. (R)-N-((R)-6-Amino-1-(4-(((2'-(isopentyloxy)-[1,1'-biphenyl]-2-yl)oxy)methyl)-1H-1,2,3-triazol-1-yl)hexan-2-yl)-5-guanidino-2-(4-(cyclohexylmethyl)-1H-1,2,3-triazol-1-yl)pentanamide dihydrochloride (**81**)*

Following **General Procedure A**, azide **75** (50 mg, 0.05 mmol), 3-cyclohexyl-1-propyne (19 mg, 0.15 mmol), $Cu(OAc)_2{\cdot}H_2O$ (2 mg, 0.01 mmol) and sodium ascorbate (4 mg, 0.02 mmol) were stirred in *t*-BuOH (1.0 mL) and H_2O (0.25 mL) for 20 h to give the intermediate triazole as a light tan gum after flash chromatography over SiO_2 gel (MeOH/CH_2Cl_2. – 0:100 → 10:90). Following **General Procedure C**, the triazole was dissolved in CH_2Cl_2 (1.5 mL) and treated with H_2O (18 mg, 1.00 mmol) and CF_3CO_2H (1.5 mL) followed by work-up with ethereal HCl to give the amine salt **81** (33 mg, 79% over two steps) as a light tan powder that rapidly transitioned to a sticky gum. $[\alpha]_D^{23}$ −23.4 (*c* 0.80, MeOH); ^{1}H NMR (400 MHz, CD_3OD) δ 7.93 (s, 1H), 7.84 (s, 1H), 7.36 – 7.24 (m, 2H), 7.23 – 7.13 (m, 3H), 7.06 – 6.91 (m, 3H), 5.34 – 5.26 (m, 1H), 5.13 (s, 2H), 4.59 (dd, *J* = 13.9, 3.8 Hz, 1H), 4.44 (dd, *J* = 13.9, 8.9 Hz, 1H), 4.27 (br s, 1H), 3.92 (t, *J* = 6.2 Hz, 2H), 3.10 (t, *J* = 6.8 Hz, 2H), 2.89 (t, *J* = 7.1 Hz, 2H), 2.61 (d, *J* = 6.8 Hz, 2H), 2.11 – 1.89 (m, 2H), 1.77 – 1.13 (m, 20H), 1.04 – 0.91 (m, 2H), 0.81 (d, *J* = 6.2 Hz, 6H); ^{13}C NMR (101 MHz, CD_3OD) δ 169.7, 158.7, 158.2, 157.5, 147.3 (observed by gHMBC), 145.8 (observed by gHMBC), 133.1, 132.7, 130.5, 129.9, 129.82, 129.76, 126.2, 124.8, 122.5, 121.5, 115.0, 113.9, 68.3, 65.2, 63.7, 54.7, 51.4, 41.7, 40.7, 39.44, 39.41, 34.2*, 33.7, 32.3, 30.4, 28.2, 27.6, 27.4*, 26.3, 26.1, 23.9, 23.1*; IR (neat) $\bar{\nu}_{max}$ 3158, 3065, 2950, 2926, 2869, 2380, 2350, 2312, 1734, 1718, 1700, 1684, 1653, 1636, 1559, 1540, 1521, 1507, 1473, 1457, 1437, 1419, 1363, 1340, 1260, 1213, 1161, 1125, 1109, 1040, 1003, 855, 750, 735, 701, 669, 608 cm^{-1}; MS (ESI +ve) *m*/2 379 ([M + 2H]$^{2+}$, 100%), *m/z* 756 ([M + H]$^+$, 19%), 778 ([M + Na]$^+$, 16%); HRMS (ESI +ve TOF) calcd for $C_{41}H_{62}N_{11}O_3$ 756.5037, found 756.5072 ([M + H]$^+$).

4.4. Microbiology assays

4.4.1. Primary screening (Gram-positive bacteria)

Primary MIC assays were performed as described by the Clinical and Laboratory Standards Institute for aerobic [36] and anaerobic [37] bacteria. *S. aureus* strains ATCC 29213 and NCTC 10442 (MRSA) and *E. faecalis* (ATCC 29212) were tested in Mueller Hinton broth (MHB) and incubation was performed in ambient air at 35 °C for 24 h. *S. pneumoniae* (ATCC 49619) was cultivated in MHB with 2.5% lysed horse blood and incubated with 5% CO_2 at 35 °C for 24 h. MIC studies for *C. difficile* strains ATCC 700057 and NSW132 (RT027) were conducted in pre-reduced (2-4 h) Brucella broth supplemented with haemin and vitamin K and incubation was performed anaerobically at 35 °C in a Don Whitley Scientific anaerobic chamber (A35) for 48 h. Each compound was dissolved in DMSO at 5 mg/mL and then diluted to 512 μg/mL with sterile, distilled water.

The compounds were then serially diluted in 100 μL volumes of sterile, distilled water in a 96-well microtitre tray. Each test organism in double strength broth (100 μL) was then added to each well and incubated as described above. Final testing concentrations of the compounds ranged from 0.25 μg/mL to 128 μg/mL. Vancomycin and a control well (i.e. no antibacterial compound present) were included in the assays. A DMSO control (5% v/v) was also tested to ensure that the solvent did not inhibit bacterial growth. The assay was performed in triplicate for each organism/compound combination and the modal MIC values were recorded. The MIC was determined visually as the lowest concentration that inhibited bacterial growth. Concentrations of ≤5% DMSO were not inhibitory to growth. MIC values for vancomycin were within acceptable QC ranges [38].

4.4.2. Secondary screening (MRSA and Gram-negative bacteria) and cytotoxicity assay – performed by the Community for Open Antimicrobial Drug Discovery (CO-ADD)

Samples were provided to CO-ADD [34] for antimicrobial screening by whole cell growth inhibition assays. The inhibition of growth was measured against five bacteria: *E. coli (*ATCC 25922), *K. pneumoniae* (ATCC 700603), *A. baumannii* (ATCC 19606), *P. aeruginosa* (ATCC 27853) and *S. aureus* (ATCC 43300). In addition to the MIC assay, compounds were screened for cytotoxicity against a human embryonic kidney cell line (HEK293) by determining their CC_{50} value. Samples were prepared in DMSO to a final testing concentration of 32 μg/mL and serially diluted 1:2 fold for 8 times. Each sample concentration was prepared in 384-well plates; non-binding surface (NBS) plates (Corning 3640) for each bacterial strain and black plates (Corning 3712/3764) for mammalian cell types, all in duplicate (n = 2) and keeping the final DMSO concentration to a maximum of 0.5%. All the sample preparation was done using liquid handling robots.

Bacterial Inhibition – MIC Assay

All bacteria were cultured in Cation-adjusted MHB at 37 °C overnight. A sample of each culture was then diluted 40-fold in fresh broth and incubated at 37 °C for 1 – 3.5 h. The resultant mid-log phase cultures were diluted (CFU/mL measured by OD_{600}), then added to each well of the compound-containing plates, giving a cell density of 5×10^5 CFU/mL and a total volume of 50 μL. All plates were covered and incubated at 37 °C for 18 h without shaking. Inhibition of bacterial growth was determined by measuring absorbance at 600 nm (OD_{600}), using a Tecan M1000 Pro monochromator plate reader. The percentage of growth inhibition was calculated for each well, using the negative control (media only) and positive control (bacteria without inhibitors) on the same plate as references. The MIC was determined as the lowest concentration at which growth was fully inhibited, defined by an inhibition ≥80%. Colistin and vancomycin were used as positive bacterial inhibitor standards for Gram-negative and Gram-positive bacteria, respectively. Each antibiotic standard was provided in four concentrations, with two above and two below its MIC value, and plated into the first eight wells of column 23 of the 384-well NBS plates.

Cytotoxicity Assay

HEK293 cells were counted manually in a Neubauer haemocytometer and then plated in the 384-well plates containing the compounds to give a density of 5000 cells/well in a final volume of 50 μL. Dulbecco's modified eagle medium (DMEM) supplemented with 10% fetal bovine serum (FBS) was used as a growth media and the cells were incubated together with the compounds for 20 h at 37 °C in 5% CO_2. Cytotoxicity (cell viability) was measured by fluorescence (ex: 560/10 nm, em: 590/10 nm), after addition of 5 μL of 25 μg/mL resazurin (2.3 μg/mL final concentration) and after incubation for further 3 h at 37 °C in 5% CO_2. The fluorescence intensity was measured using a Tecan M1000 Pro monochromator plate reader, using automatic gain calculation. CC_{50} (concentration at 50% cytotoxicity) values were calculated by curve-fitting the inhibition values vs. log(concentration) using a sigmoidal dose-response function, with variable fitting values for bottom, top and slope. Tamoxifen was utilized as a positive cytotoxicity standard; it was used in eight concentrations in two-fold serial dilutions with 50 μg/mL as the highest concentration tested.

4.4.3. Extended panel screening (drug resistant Gram-positive bacteria) – performed by the Community for Open Antimicrobial Drug Discovery (CO-ADD)

Extended panel MIC assays were performed by CO-ADD as per section 4.4.2 against the following bacterial strains: *S. aureus* ATCC 43300 (MRSA), *S. aureus* clinical isolate (MRSA), *S. aureus* NRS17 (GISA),

S. aureus NRS1 (GISA/MRSA), *S. aureus* clinical isolate (MRSA/reduced daptomycin susceptibility), *S. aureus* VRS10 – NARSA (VRSA), *S. pneumoniae* ATCC700677 (MDR), and *E. faecalis* clinical isolate (VRE). Vancomycin and daptomycin were used as positive bacterial inhibitor standards.

4.4.4. Haemolysis assay

The haemolytic activity of the synthesized compounds was determined by lysis of sheep erythrocytes. Briefly, 500 µL volumes of each compound in phosphate buffer solution (PBS) were mixed with 480 µL PBS and 20 µL washed sheep erythrocytes (100%) in microcentrifuge tubes; this produced a final erythrocyte concentration of 2%. Compounds were tested at both 5 µg/mL and 50 µg/mL. A positive control (980 µL water and 20 µL erythrocytes) and a negative control (980 µL PBS and 20 µL erythrocytes) were also included in the assay. The centrifuge tubes were incubated on a rocker at 37 °C for 2 h and then centrifuged at 12,000 rpm for 5 min; 100 µL volumes of the supernatant fluid were transferred to a 96-well microtitre tray and the optical density of the samples was observed at 540 nm. The value for the negative control was subtracted from the haemolysis values and then the resulting quantities were expressed as a percentage of the positive control (which was defined as 100% haemolysis). The haemolysis assay was repeated in triplicate for all compounds and the mean values were reported.

4.4.5. Time-kill kinetics assay

A 100 µl aliquot of a 0.5 McFarland standard of *S. aureus* ATCC 29213 or *E. coli* ATCC 25922 was inoculated in 20 mL of MHB and incubated at 37 °C for 18 h ('overnight culture'). The overnight culture was diluted 1 in 1,000 in MHB. For each organism, three 5 mL aliquots were prepared in 10 mL tubes. The tubes were incubated at 37 °C, lid loose, with aeration (225 rpm) for 2 h (early exponential phase). The bacterial cultures were then challenged with compound **71** at 64 µg/mL (8–16 × MIC) and incubation was continued at 37 °C, lid loose, with aeration (225 rpm). A 100 µL aliquot was taken from each tube before the challenge (T=0), 30 min after challenge, 60 min after the challenge and then at 1 h intervals until total time = 6 h. Ten-fold serially diluted suspensions of each 100 µL aliquot were plated onto pre-dried blood agar plates. The blood agar plates were incubated for 18 h at 37 °C. Colonies were counted and CFU/mL were calculated. UltraPure H_2O was utilized as a negative control for both species. Vancomycin (8 µg/mL) was used as an antibiotic control for *S. aureus* and colistin (4 µg/mL) was used as an antibiotic control for *E. coli*. The limit of detection = 10^3 CFU/mL.

4.4.6. Cytoplasmic membrane depolarization assay

An inoculum containing 1.5 McFarland standard of mid-log cells (*S. aureus* ATCC 29213 or *E. coli* NCTC 10418) was suspended in either phosphate buffered saline (PBS – for *S. aureus*) or a 5 mM HEPES solution containing 20 mM glucose adjusted to pH 7.2 (for *E. coli*). Then, 3,3′-dipropylthiadicarbocyanine ($diSC_3(5)$) was added at 4 µM to the bacteria suspension and the mixture was incubated in the dark at room temperature (30 min for *S. aureus* and 60 min for *E. coli*). For *E. coli* only, KCl was then added at 100 mM, followed by EDTA at 0.5 mM. Then, 100 µL aliquots of the bacterial suspension were added to wells of a 96-well plate (black with clear bottom); the fluorescence was tracked (ex: 620/10 nm, em: 670/10 nm) for approximately 8 min prior to exposure to the test compounds. The content of each well was then transferred to a different well containing 100 µL of one of the various test compounds prepared at double the final test concentration. The fluorescence was then tracked for approximately 30 min. The final assay concentration of the test compounds was 32 µg/mL for *S. aureus* and 64 µg/mL for *E. coli*. UltraPure H_2O was utilized as a negative control for both species. DMSO (20%) was utilized as a positive control for both species. Vancomycin (8 µg/mL) was used as a negative control for *S. aureus* and colistin (64 µg/mL) was used as positive control for *E. coli*.

4.4.7. Cytoplasmic membrane permeabilization assay

An inoculum containing 1.5 McFarland standard of mid-log cells (*S. aureus* ATCC 29213 or *E. coli* NCTC 10418) was suspended in either phosphate buffered saline (PBS – for *S. aureus*) or a 5 mM HEPES solution containing 20 mM glucose adjusted to pH 7.2 (for *E. coli*). Then, propidium iodide was added at 4 µM to the bacteria suspension and the mixture was incubated in the dark at room temperature (30 min for *S. aureus*

and 60 min for *E. coli*). For *E. coli* only, KCl was then added at 100 mM, followed by EDTA at 0.5 mM. Then, 100 µL aliquots of the bacterial suspension were added to wells of a 96-well plate (black with clear bottom); the fluorescence was tracked (ex: 544/10 nm, em: 615/10 nm) for approximately 8 min prior to exposure to the test compounds. The content of each well was then transferred to a different well containing 100 µL of one of the various test compounds prepared at double the final test concentration. The fluorescence was then tracked for approximately 30 min. The final assay concentration of the test compounds was 32 µg/mL for both *S. aureus* and *E. coli*. UltraPure H_2O was utilized as a negative control for both species. Vancomycin (8 µg/mL) was used as a negative control for *S. aureus* and colistin (64 µg/mL) was used as a positive control for *E. coli*.

Acknowledgements

The authors thank the Australian National Health and Medical Research Council (NHMRC) for financial support (Grant #APP1124032). The authors are grateful for antimicrobial screening that was performed by CO-ADD (The Community for Antimicrobial Drug Discovery), funded by the Wellcome Trust (UK) and The University of Queensland (Australia).

Declarations of Interest

The authors declare no competing financial interests.

Appendix A. Supplementary information

Supplementary information related to this article can be found online at https://doi.org/xxxxxxx.

References

1. World Health Organization. Antibiotic Resistance Fact Sheet. http://www.who.int/mediacentre/factsheets/antibiotic-resistance/en/ (accessed June 12th, 2018).

2. Centers for Disease Control. Antibiotic/Antimicrobial Resistance. https://www.cdc.gov/drugresistance/ (accessed June 12th, 2018)

3. Roca, I.; Akova, M.; Baquero, F.; Carlet, J.; Cavaleri, M.; Coenen, S.; Cohen, J.; Findlay, D.; Gyssens, I.; Heure, O. E.; *et al*. The global threat of antimicrobial resistance: science for intervention. *New Microbes New Infect.* **2015**, *6*, 22-9.

4. Pourmand, A.; Mazer-Amirshahi, M.; Jasani, G.; May, L. Emerging trends in antibiotic resistance: Implications for emergency medicine. *Am. J. Emerg. Med.* **2017**, *35* (8), 1172-1176.

5. Martens, E.; Demain, A. L. The antibiotic resistance crisis, with a focus on the United States. *J. Antibiot.* **2017**, *70* (5), 520-526.

6. Pendleton, J. N.; Gorman, S. P.; Gilmore, B. F. Clinical relevance of the ESKAPE pathogens. *Expert Review of Anti-infective Therapy* **2013**, *11* (3), 297-308.

7. Penchovsky, R.; Traykovska, M. Designing drugs that overcome antibacterial resistance: where do we stand and what should we do? *Expert. Opin. Drug Discov.* **2015**, *10* (6), 631-650.

8. Ghosh, C.; Haldar, J. Membrane-Active Small Molecules: Designs Inspired by Antimicrobial Peptides. *ChemMedChem* **2015**, *10* (10), 1606-1624.

9. Herzog, I. M.; Fridman, M. Design and synthesis of membrane-targeting antibiotics: from peptides-to aminosugar-based antimicrobial cationic amphiphiles. *MedChemComm* **2014**, *5* (8), 1014-1026.

10. Molchanova, N.; Hansen, P. R.; Franzyk, H. Advances in Development of Antimicrobial Peptidomimetics as Potential Drugs. *Molecules (Basel, Switzerland)* **2017**, *22* (9), 1430.

11. Hein-Kristensen, L.; Franzyk, H.; Holch, A.; Gram, L. Adaptive Evolution of Escherichia coli to an α-Peptide/β-Peptoid Peptidomimetic Induces Stable Resistance. *PLOS ONE* **2013**, *8* (9), e73620.

12. Ghosh, C.; Manjunath, G. B.; Akkapeddi, P.; Yarlagadda, V.; Hoque, J.; Uppu, D.; Konai, M. M.; Haldar, J. Small Molecular Antibacterial Peptoid Mimics: The Simpler the Better! *Journal of Medicinal Chemistry* **2014**, *57* (4), 1428-1436.

13. Kuppusamy, R.; Yasir, M.; Berry, T.; Cranfield, C. G.; Nizalapur, S.; Yee, E.; Kimyon, O.; Taunk, A.; Ho, K. K. K.; Cornell, B.; Manefield, M.; Willcox, M.; Black, D. S.; Kumar, N. Design and synthesis of short amphiphilic cationic peptidomimetics based on biphenyl backbone as antibacterial agents. *European Journal of Medicinal Chemistry* **2018**, *143*, 1702-1722.

14. Wales, S. M.; Hammer, K. A.; King, A. M.; Tague, A. J.; Lyras, D.; Riley, T. V.; Keller, P. A.; Pyne, S. G. Binaphthyl-1,2,3-triazole peptidomimetics with activity against *Clostridium difficile* and other pathogenic bacteria. *Org. Biomol. Chem.* **2015**, *13* (20), 5743-5756.

15. Wales, S. M.; Hammer, K. A.; Somphol, K.; Kemker, I.; Schroder, D. C.; Tague, A. J.; Brkic, Z.; King, A. M.; Lyras, D.; Riley, T. V.; Bremner, J. B.; Keller, P. A.; Pyne, S. G., Synthesis and antimicrobial activity of binaphthyl-based, functionalized oxazole and thiazole peptidomimetics. *Org. Biomol. Chem.* **2015**, *13* (44), 10813-10824.

16. Lin, S.; Koh, J.-J.; Aung, T. T.; Lim, F.; Li, J.; Zou, H.; Wang, L.; Lakshminarayanan, R.; Verma, C.; Liu, S.; *et al*. Symmetrically Substituted Xanthone Amphiphiles Combat Gram-Positive Bacterial Resistance with Enhanced Membrane Selectivity. *J. Med. Chem.* **2017**, *60* (4), 1362-1378.

17. Chu, W.-C.; Bai, P.-Y.; Yang, Z.-Q.; Cui, D.-Y.; Hua, Y.-G.; Yang, Y.; Yang, Q.-Q.; Zhang, E.; Qin, S. Synthesis and antibacterial evaluation of novel cationic chalcone derivatives possessing broad spectrum antibacterial activity. *Eur. J. Med. Chem.* **2018**, *143*, 905-921.

18. Zhang, E.; Bai, P.-Y.; Cui, D.-Y.; Chu, W.-C.; Hua, Y.-G.; Liu, Q.; Yin, H.-Y.; Zhang, Y.-J.; Qin, S.; Liu, H.-M. Synthesis and bioactivities study of new antibacterial peptide mimics: The dialkyl cationic amphiphiles. *Eur. J. Med. Chem.* **2018**, *143*, 1489-1509.

19. Vooturi, S. K.; Dewal, M. B.; Firestine, S. M. Examination of a synthetic benzophenone membrane-targeted antibiotic. *Org. Biomol. Chem.* **2011**, *9* (18), 6367-6372.

20. Ahn, M.; Gunasekaran, P.; Rajasekaran, G.; Kim, E. Y.; Lee, S.-J.; Bang, G.; Cho, K.; Hyun, J.-K.; Lee, H.-J.; Jeon, Y. H.; Kim, N.-H.; Ryu, E. K.; Shin, S. Y.; Bang, J. K. Pyrazole derived ultra-short antimicrobial peptidomimetics with potent anti-biofilm activity. *Eur. J. Med. Chem.* **2017**, *125*, 551-564.

21. Lai, X.-Z.; Feng, Y.; Pollard, J.; Chin, J. N.; Rybak, M. J.; Bucki, R.; Epand, R. F.; Epand, R. M.; Savage, P. B. Ceragenins: Cholic Acid-Based Mimics of Antimicrobial Peptides. *Accounts Chem. Res.* **2008**, *41* (10), 1233-1240.

22. Nilsson, A. C.; Janson, H.; Wold, H.; Fugelli, A.; Andersson, K.; Håkangård, C.; Olsson, P.; Olsen, W. M. LTX-109 Is a Novel Agent for Nasal Decolonization of Methicillin-Resistant and -Sensitive *Staphylococcus aureus*. *Antimicrob. Agents Chemother.* **2015**, *59* (1), 145-151.

23. Isaksson, J.; Brandsdal, B. O.; Engqvist, M.; Flaten, G. E.; Svendsen, J. S. M.; Stensen, W. A Synthetic Antimicrobial Peptidomimetic (LTX 109): Stereochemical Impact on Membrane Disruption. *J. Med. Chem.* **2011**, *54* (16), 5786-5795.

24. Hoque, J.; Konai, M. M.; Sequeira, S. S.; Samaddar, S.; Haldar, J. Antibacterial and Antibiofilm Activity of Cationic Small Molecules with Spatial Positioning of Hydrophobicity: An *in Vitro* and *in Vivo* Evaluation. *J. Med. Chem.* **2016**, *59* (23), 10750-10762.

25. O'Neill, A. New antibacterial agents for treating infections caused by multi-drug resistant Gram-negatve bacteria. *Expert Opin. Investig. Drugs* **2008**, *17* (3), 297-302.

26. Bremner, J. B.; Keller, P. A.; Pyne, S. G.; Boyle, T. P.; Brkic, Z.; David, D. M.; Garas, A.; Morgan, J.; Robertson, M.; Somphol, K.; *et al*. Binaphthyl-Based Dicationic Peptoids with Therapeutic Potential. *Angew. Chem.-Int. Edit.* **2010**, *49* (3), 537-540.

27. Bremner, J. B.; Keller, P. A.; Pyne, S. G.; Boyle, T. P.; Brkic, Z.; David, D. M.; Robertson, M.; Somphol, K.; Baylis, D.; Coates, J. A.; *et al*. Synthesis and antibacterial studies of binaphthyl-based tripeptoids. Part 1. *Bioorg. Med. Chem.* **2010**, *18* (7), 2611-2620.

28. Bremner, J. B.; Keller, P. A.; Pyne, S. G.; Boyle, T. P.; Brkic, Z.; Morgan, J.; Somphol, K.; Coates, J. A.; Deadman, J.; Rhodes, D. I. Synthesis and antibacterial studies of binaphthyl-based tripeptoids. Part 2. *Bioorg. Med. Chem.* **2010**, *18* (13), 4793-4800.

29. Garas, A.; Bremner, J. B.; Coates, J.; Deadman, J.; Keller, P. A.; Pyne, S. G.; Rhodes, D. I. Binaphthyl scaffolded peptoids *via* ring-closing metathesis reactions and their anti-bacterial activities. *Bioorg. Med. Chem. Lett.* **2009**, *19* (11), 3010-3013.

30. Khara, J. S.; Priestman, M.; Uhía, I.; Hamilton, M. S.; Krishnan, N.; Wang, Y.; Yang, Y. Y.; Langford, P. R.; Newton, S. M.; Robertson, B. D.; Ee, P. L. R. Unnatural amino acid analogues of membrane-active helical peptides with anti-mycobacterial activity and improved stability. *J. Antimicrob. Chemother.* **2016**, *71* (8), 2181-2191.

31. Boyle, T. P.; Bremner, J. B.; Brkic, Z.; Coates, J. A. V.; Dalton, N. K.; Deadman, J.; Keller, P. A.; Morgan, J.; Pyne, S. G.; Rhodes, D. I.; Robertson, M. J. Preparation of biaryl-based peptides for the treatment of infection. WO2006074501A1, 2006.

32. Rodionov, V. O.; Fokin, V. V.; Finn, M. G. Mechanism of the ligand-free Cu-I-catalyzed azide-alkyne cycloaddition reaction. *Angew. Chem.-Int. Edit.* **2005**, *44* (15), 2210-2215.

33. Rodionov, V. O.; Presolski, S. I.; Díaz Díaz, D.; Fokin, V. V.; Finn, M. G. Ligand-Accelerated Cu-Catalyzed Azide−Alkyne Cycloaddition: A Mechanistic Report. *J. Am. Chem. Soc.* **2007**, *129* (42), 12705-12712.

34. Rostovtsev, V. V.; Green, L. G.; Fokin, V. V.; Sharpless, K. B. A stepwise Huisgen cycloaddition process: Copper(I)-catalyzed regioselective "ligation" of azides and terminal alkynes. *Angew. Chem.-Int. Edit.* **2002**, *41* (14), 2596.

35. Blaskovich, M. A. T.; Zuegg, J.; Elliott, A. G.; Cooper, M. A. Helping Chemists Discover New Antibiotics. *ACS Infect. Dis.* **2015**, *1* (7), 285-287.

36. Clinical and Laboratory Standards Institute. Methods for Dilution Antimicrobial Susceptibility Tests for Bacteria That Grow Aerobically; Approved Standard – Ninth Edition. **2015**. CLSI Document M07-A10. *Clinical and Laboratory Standards Institute*, Wayne, Pennsylvania.

37. Clinical and Laboratory Standards Institute. Methods for Antimicrobial Susceptibility Testing of Anaerobic Bacteria; Approved Standard – Eighth Edition. **2012**. CLSI Document M11-A8. *Clinical and Laboratory Standards Institute*, Wayne, Pennsylvania.

38. Clinical Laboratory Standards Institute. Performance Standards for Antimicrobial Susceptibility Testing, 28th Informational Supplement. **2018**. CLSI document M100-S28. *Clinical and Laboratory Standards Institute*, Wayne, Pennsylvania.

Highlights

- Synthesis of 43 cationic biaryl 1,2,3-triazolyl peptidomimetic amphiphiles
- Modular and facile synthetic access to a diverse range of peptidomimetic scaffolds
- Potent broad-spectrum *in vitro* efficacy against drug-resistant pathogenic bacteria
- Membrane disruption assays indicate a membrane-active mechanism